SMAI-JCM
SMAI Journal of Computational Mathematics

Electrostatic Force Computation with Boundary Element Methods

Piyush Panchal & Ralf Hiptmair

Volume 8 (2022), p. 49-74.

<http://smai-jcm.centre-mersenne.org/item?id=SMAI-JCM_2022__8__49_0>

Publication membre du
Centre Mersenne pour l'édition scientifique ouverte
http://www.centre-mersenne.org/

Soumission sur https://smai-jcm.centre-mersenne.org/ojs/submission

SMAI Journal of Computational Mathematics
Vol. 8, 49-74 (2022)

Electrostatic Force Computation with Boundary Element Methods

Piyush Panchal [1]
Ralf Hiptmair [2]

[1] SAM, D-MATH, ETH Zurich, CH-8092 Zürich
E-mail address: piyush.panchal@sam.math.ethz.ch
[2] SAM, D-MATH, ETH Zurich, CH-8092 Zürich
E-mail address: hiptmair@sam.math.ethz.ch.

Abstract. Boundary element methods are a well-established technique for solving linear boundary value problems for electrostatic potentials. In this context we present a novel way to approximate the forces exerted by electrostatic fields on conducting objects. Like the standard post-processing technique employing surface integrals derived from the Maxwell stress tensor the new approach solely relies on surface integrals, but, compared to the former, offers better accuracy and faster convergence.

The new formulas arise from the interpretation of forces fields as shape derivatives, in the spirit of the virtual work principle, combined with the adjoint approach from shape optimization. In contrast to standard formulas, they meet the continuity and smoothing requirements of abstract duality arguments, which supply a rigorous underpinning for their observed superior performance.

2020 Mathematics Subject Classification. 65N38, 78M15, 45A05.

Keywords. Electrostatics, electromagnetic forces, shape derivative, boundary integral equations, boundary element method.

1. Introduction

1.1. Model Problem

A solid conducting object filling the bounded open connected Lipschitz domain $D \subset \mathbb{R}^d$, $d = 2, 3$, is embedded in a non-conducting homogeneous isotropic dielectric medium. Both together occupy a larger bounded open Lipschitz domain $B \subset \mathbb{R}^d$, $\overline{D} \subset B$, which represents the geometry of a container with metal walls.

A potential difference U is imposed between the object and the metal box by a voltage source, see Figure 1.1. For $d = 3$ this arrangement represents a realistic laboratory setup, for $d = 2$ it is to be read as a cross-section description of a situation with translational symmetry. We use the short notations $\Omega := B \setminus \overline{D}$ for the "field domain", $\Gamma := \partial D$ for the boundary of the object, and assume that Γ is connected.

The (non-dimensional, rescaled) electrostatic scalar potential $u : \Omega \to \mathbb{R}$ can be obtained as the unique weak solution in $H^1(\Omega)$[1] of the linear elliptic boundary value problem

$$\Delta u = 0 \quad \text{in} \quad \Omega \quad , \quad u = 0 \quad \text{on} \quad \partial B \, , \quad u = g \quad \text{on} \quad \Gamma := \partial D \, . \tag{1.1}$$

The physical setting of Figure 1.1 corresponds to constant Dirichlet data $g \equiv U$, but we prefer to admit general $g \in H^{\frac{1}{2}}(\partial\Omega)$ at this point.

Remark 1.1. The model problem was chosen for the sake of simplicity. We emphasize that the ideas and techniques pursued in this work can straightforwardly be extended to the situation of two conducting objects in free space, with either a potential drop imposed between them (Figure 1.2, left) or some total electric charges put on them (Figure 1.2, right).

[1] We use standard notations for function spaces and, in particular, Sobolev spaces: $C^\infty(\Omega)$, $L^2(\Omega)$, $H^s(\Omega)$, $W^{m,\infty}(\Omega)$, etc., where Ω denotes a "generic domain". We adopt the conventions of [28, Sect 2.3 & 2.4].

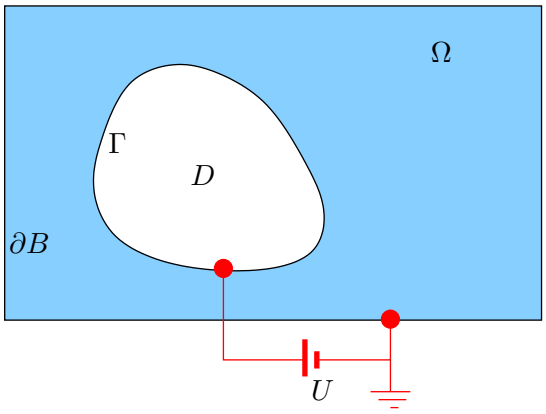

FIGURE 1.1. Geometric setting for model problem

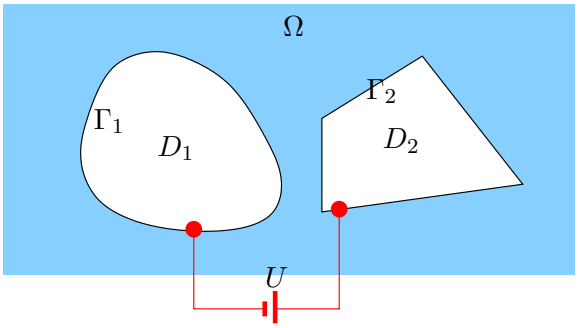

(A) Imposed potential difference

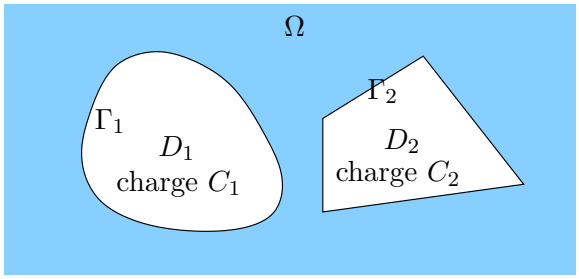

(B) Fixed total charge

FIGURE 1.2. More general arrangements of conducting objects in free space $\mathbb{R}^d$

1.2. **Classical Formulas for Electrostatic Forces**

This work is concerned with a new numerical method for computing the total force, torque, as well as surface forces acting on the object. We remind that standard methods employ the Maxwell stress tensor[2] [22, §6.9]

$$\mathbf{T}(u) := \boldsymbol{\nabla} u \boldsymbol{\nabla} u^\top - \frac{1}{2}\|\boldsymbol{\nabla} u\|^2 \mathbf{I}_d : \Omega \to \mathbb{R}^{d,d} , \tag{1.2}$$

involving the electrostatic potential u, which solves (1.1). Then, writing $\boldsymbol{n}$ for the exterior unit normal vector field on $\partial\Omega$, the vector field $\mathbf{f}^\Gamma(\boldsymbol{x}) := \mathbf{T}(u(\boldsymbol{x}))\boldsymbol{n}(\boldsymbol{x})$, $\boldsymbol{x} \in \Gamma$. gives the electrostatic surface force density, and, consequently,

$$\mathbf{F} := \int_\Gamma \mathbf{f}^\Gamma \,\mathrm{d}S = \int_\Gamma \mathbf{T}(u)\boldsymbol{n} \,\mathrm{d}S = \frac{1}{2}\int_\Gamma |\boldsymbol{\nabla} u \cdot \boldsymbol{n}|^2 \boldsymbol{n} \,\mathrm{d}S \tag{1.3}$$

is the total force on the object, where the last equality holds for constant Dirichlet data $g \equiv U$. Since $\boldsymbol{\nabla} \cdot \mathbf{T}(u) = \mathbf{0}$, by elementary computations using $\Delta u = 0$, integration by parts yields the *equivalent* formula [3]

$$\mathbf{F} = \int_\Omega \mathbf{T}(u)\boldsymbol{\nabla} w \,\mathrm{d}\boldsymbol{x} = \int_\Omega \boldsymbol{\nabla} u(\boldsymbol{\nabla} u \cdot \boldsymbol{\nabla} w) - \frac{1}{2}\|\boldsymbol{\nabla} u\|^2 \boldsymbol{\nabla} w \,\mathrm{d}\boldsymbol{x} . \tag{1.4}$$

[2] $\mathbf{I}_d$ stands for the $d \times d$ identity matrix.
[3] We write $\cdot$ for the inner product in Euclidean space $\mathbb{R}^d$ and $\|\cdot\|$ for the associated norm.

for *any* $w \in W^{1,\infty}(\Omega)$ with $w|_\Gamma \equiv 1$ and $w|_{\partial B} \equiv 0$.

Experiment 1. We solved (1.1) for $g \equiv 1$ by means of piecewise linear C^0 finite elements on quasi-uniform shape-regular sequences of triangular meshes for $d = 2$, and

(i) a smooth "kite-shaped" D, given by the parameterization $\gamma : [0, 2\pi] \to \mathbb{R}^2$, $t \mapsto [0.3 + 0.35\cos(t) + 0.1625\cos(2t), 0.5 + 0.35\sin(t)]$ and a square-shaped $B =]-2, 2[\times]-2, 2[$, and

(ii) a unit square $D :=]0, 1[^2$ inside $B :=]-3, 3[\times]-3, 3[$.

The coarsest meshes used for each geometry are displayed in Figure 1.3.

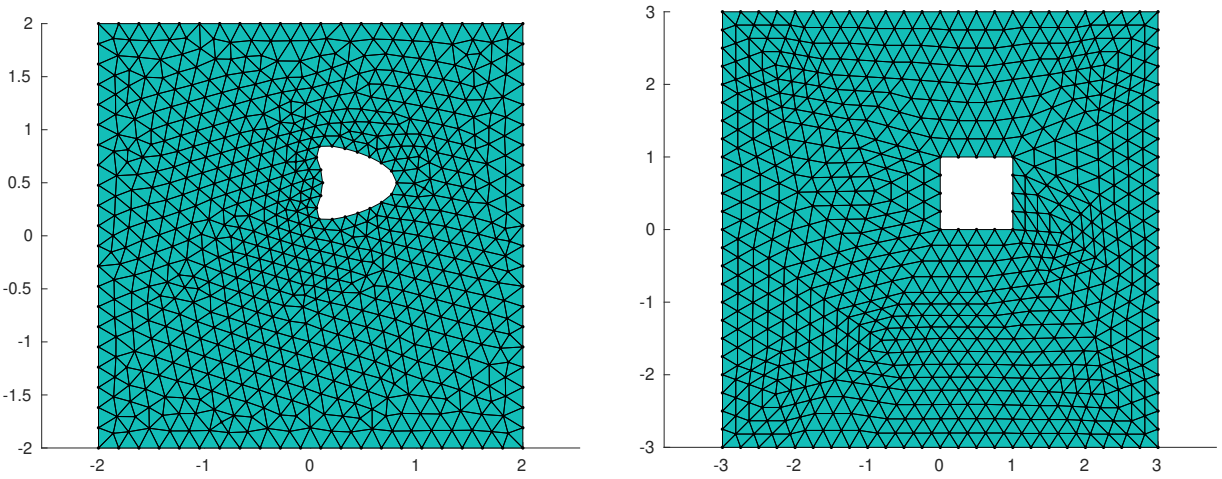

(A) Kite-shaped D (B) Square-shaped D

Figure 1.3. Geometries and coarsest finite element meshes for the numerical tests covered in Experiment 1

We directly evaluate both formulas for the finite element solution and use the following C^1 cut-off function in the volume-based formula (1.4):

$$w(\boldsymbol{x}) := \begin{cases} 1 & \text{for } \|\boldsymbol{x}\| < 1.2 \,, \\ \cos^2\left(\frac{\|\boldsymbol{x}\|-1.2}{0.7}\right) & \text{for } 1.2 \le \|\boldsymbol{x}\| \le 1.9 \,, \\ 0 & \text{for } \|\boldsymbol{x}\| > 1.9 \,, \end{cases} \tag{1.5}$$

The Euclidean norm of the error in the computed forces is shown in Figure 1.4 as a function of the mesh width h of the underlying triangulations. [4]

We make the striking observation that, when used with a finite-element solution, the volume-based formula (1.4) enjoys a vast superiority over the boundary-based formula (1.3), both in terms of absolute accuracy and in terms of rate of asymptotic (algebraic) convergence.

[4] As reference solution we used the total force computed by the pullback approach (4.17) on a uniform mesh with 9000 (kite-shaped D)/7200 (square-shaped D) cells

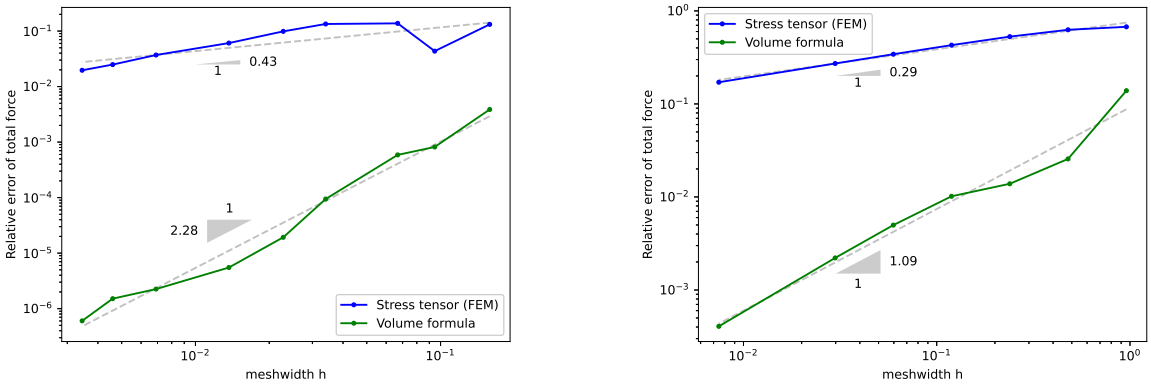

(A) Kite-shaped D

(B) Square-shaped D

FIGURE 1.4. Euclidean norm of errors in approximate total force for finite-element solution inserted into (1.3) (blue, "Stress tensor (FEM)") and (1.4) (green, "Volume formula"), respectively. The dashed lines represent the linear regression fit.

1.3. **Benefits of Smoothness**

Duality arguments will shed light on the surprising outcome of Experiment 1. We start from the variational formulation of (1.1) in the Sobolev space $V := H^1(\Omega)$:

$$u \in V_g := H^1_0(\Omega) + \widetilde{g} : \quad \mathsf{a}(u,v) := \int_\Omega \boldsymbol{\nabla} u \cdot \boldsymbol{\nabla} v \,\mathrm{d}\boldsymbol{x} = 0 \quad \forall v \in V_0 := H^1_0(\Omega) \,, \tag{1.6}$$

where $\widetilde{g} \in H^1(\Omega)$ extends the Dirichlet data g, $\widetilde{g}|_\Gamma = g$, and vanishes on ∂B. Let $V_{0,h} \subset V_0$ denote an $H^1(\Omega)$-conforming finite-element space. Ignoring potentially necessary approximations of $\widetilde{g}$, the finite-element solution u_h is obtained as

$$u_h \in V_{g,h} := V_{0,h} + \widetilde{g} : \quad \mathsf{a}(u_h, v_h) = 0 \quad \forall v_h \in V_{0,h} \,. \tag{1.7}$$

Following [1, §2.1] let $F : V \to \mathbb{R}$ be a *twice continuously differentiable* "output" functional. We write $\mathsf{D}^\ell F$, $\ell = 1, 2$, for its ℓ-th derivative, which is a continuous mapping from Ω into the ℓ-multilinear forms on V. Now, essentially keeping the notations, we switch to a more abstract setting.

Proposition 1.2. *Let $V_{0,h} \subset V_0 \subset V$ be closed subspaces of a Banach space V, and let $\mathsf{a} : V \times V \to \mathbb{R}$ be a bounded V_0-elliptic bilinear form, $\ell \in V'$, $\widetilde{g} \in V$, and consider the variational problems*

$$u \in V_0 + \widetilde{g} : \qquad \mathsf{a}(u,v) = \ell(v) \quad \forall v \in V_0 \,, \tag{1.8}$$

$$u_h \in V_{0,h} + \widetilde{g} : \qquad \mathsf{a}(u_h, v_h) = \ell(v_h) \quad \forall v_h \in V_{0,h} \,. \tag{1.9}$$

If $F \in C^2(V, \mathbb{R})$, then the output error estimate[5]

$$|F(u) - F(u_h)| \le \|\mathsf{a}\| \, \|u - u_h\|_V \inf_{v_h \in V_{0,h}} \|z - v_h\|_V + \frac{1}{2} \max_{0 \le \tau \le 1} \left\| \mathsf{D}^2 F(\tau u_h + (1-\tau)u) \right\| \, \|u - u_h\|_V^2 \tag{1.10}$$

holds true, where u, u_h designate the solutions of (1.8) and (1.9), respectively, and $z \in V_0$ is the solution of the adjoint variational problem

$$z \in V_0 : \quad \mathsf{a}(v,z) = \mathsf{D}F(u)(v) \quad \forall v \in V_0 \,. \tag{1.11}$$

[5] $\|\mathsf{a}\|$ and $\left\|\mathsf{D}^2 F\right\|$ designate the operator norms of bounded bilinear mappings $V \times V \to \mathbb{R}$

Proof. By the Lax-Milgram lemma [5, §6.2] existence and uniqueness of both u and u_h is guaranteed. We write $e := u_h - u \in V_0$ for the Galerkin discretization error and recall its property known as Galerkin orthogonality: $\mathsf{a}(e, v_h) = 0$ for all $v_h \in V_{0,h}$. By second-order Taylor expansion [5, Thm. 7.9-1] we find

$$F(u+e) - F(u) = \mathsf{D}F(u)(e) + \int_0^1 (1-t)\mathsf{D}^2F(u+te)(e,e)\,\mathrm{d}t\,. \tag{1.12}$$

Thanks to the defining equation (1.11) for $z \in V_0$ and Galerkin orthogonality, we can rewrite

$$\mathsf{D}F(u)(e) = \mathsf{a}(e,z) = \mathsf{a}(e, z - v_h) \quad \forall v_h \in V_{0,h}\,. \tag{1.13}$$

The continuity estimate $|\mathsf{a}(v,v')| \leq \|\mathsf{a}\|\,\|v\|_V\,\|v'\|_V$ for all $v, v' \in V_0$ together with the definition of the norm of D^2F finishes the proof. ∎

For the h-version of the finite-element method (FEM) the message of Proposition 1.2 is that the output error $F(u) - F(u_h)$ can converge to zero faster than the energy norm $\|u - u_h\|_V$ of the Galerkin discretization error provided that the best-approximation error $\inf_{v_h \in V_{0,h}} \|z - v_h\|_V$ for the solution z of the adjoint variational problem tends to zero with some rate. In this case we observe *superconvergence* of $F(u_h) \to F(u)$ for $h \to 0$.

Proposition 1.2 is key to understanding Experiment 1: The boundary-based output functional (1.3) is not even continuous on $H^1(\Omega)$, let alone differentiable. We conclude this from the failure of the co-normal trace $u \mapsto \boldsymbol{\nabla} u \cdot \boldsymbol{n}|_\Gamma$ to map from $H^1(\Omega)$ into $L^2(\Gamma)$. Conversely, if $w \in W^{1,\infty}(\Omega)$, then the volume-based functional (1.4) is a smooth quadratic functional on $H^1(\Omega)$. If $w \in W^{2,\infty}(\Omega)$ as in Experiment 1 and $u \in H^2(\Omega)$, then the first derivative of the volume-based force functional will even be continuous on $L^2(\Omega)$, which entails extra smoothness of the dual solution z by virtue of elliptic lifting results. This explains the "superconvergence" of the forces computed by means of (1.4) in Experiment 1.

Remark 1.3. In computational engineering the use of a volume-based formula for the computation of electromagnetic forces on bounded objects is known as the "eggshell method" [17, 15, 24].

1.4. **Outline and Novelty**

In this work we harness the superconvergence afforded by the duality arguments of Proposition 1.2 by means of new formulas for electrostatic forces that exclusively rely on integration over $\partial\Omega$. These formulas are based on the virtual work principle that offers a natural interpretation of force fields as shape derivatives. We have elaborated this idea in Section 3. The actual derivation of the new formulas is presented in Section 4.1 and Section 4.2. It relies on the reformulation of the boundary value problem (1.1) as a weakly singular first-kind boundary integral equation (BIE) in Section 2.1, the adjoint method borrowed from constrained optimization, and an idea we introduce as "pullback approach". Forces are then approximated using boundary element Galerkin solutions of the BIEs in variational form, see Section 4.3. In Section 4.4 we confirm that we can expect the extra regularities required for the superconvergence of approximate forces. This superconvergence clearly manifests itself in the numerical experiments reported in Section 5.

2. **Boundary Element Method (BEM)**

For the numerical solution of the boundary value problem (1.1) we opt for a low-order boundary-element Galerkin discretization based on a direct first-kind boundary integral equation. As regards this widely used standard method we just refer to the textbooks [28, Ch. 3 & 4] and [30, Ch. 6–8]. There the reader can also find information about the trace space $H^{\frac{1}{2}}(\partial\Omega)$ and its dual space $H^{-\frac{1}{2}}(\partial\Omega)$.

2.1. **Variational Boundary Integral Equations (BIEs)**

From [28, §2.9.2.1], [25, Thm. 7.5] we learn that the unknown co-normal/Neumann trace $\psi := \boldsymbol{\nabla} u \cdot \boldsymbol{n}|_{\partial\Omega}$ of the solution of (1.1) can be recovered as the solution of the following first-kind boundary integral equation

$$\psi \in H^{-\frac{1}{2}}(\partial\Omega): \quad \mathsf{a}_V(\psi,\varphi) = \frac{1}{2}\ell_g(\varphi) + \mathsf{b}_K(g,\varphi) \quad \forall \varphi \in H^{-\frac{1}{2}}(\partial\Omega)\,, \tag{2.1}$$

with

$$\begin{aligned} \mathsf{a}_V(\psi,\varphi) &:= \int_{\partial\Omega}\int_{\partial\Omega} G(\boldsymbol{x},\boldsymbol{y})\,\psi(\boldsymbol{y})\,\varphi(\boldsymbol{x})\,\mathrm{d}S(\boldsymbol{y})\mathrm{d}S(\boldsymbol{x})\,,\\ \mathsf{b}_K(g,\varphi) &:= \int_{\partial\Omega}\int_{\partial\Omega} \boldsymbol{\nabla}_{\boldsymbol{y}} G(\boldsymbol{x},\boldsymbol{y})\cdot\boldsymbol{n}(\boldsymbol{y})\,g(\boldsymbol{y})\,\varphi(\boldsymbol{x})\,\mathrm{d}S(\boldsymbol{y})\mathrm{d}S(\boldsymbol{x})\,,\\ \ell_g(\varphi) &:= \int_{\partial\Omega} g(\boldsymbol{x})\,\varphi(\boldsymbol{x})\,\mathrm{d}S(\boldsymbol{x})\,, \end{aligned} \tag{2.2}$$

and the fundamental solutions $G : \{(\boldsymbol{x},\boldsymbol{y}) \in \mathbb{R}^d \times \mathbb{R}^d,\, \boldsymbol{x} \neq \boldsymbol{y}\} \to \mathbb{R}$

$$G(\boldsymbol{x},\boldsymbol{y}) := -\frac{1}{2\pi}\log(\|\boldsymbol{x}-\boldsymbol{y}\|) \quad \text{for } d=2 \quad , \quad G(\boldsymbol{x},\boldsymbol{y}) := \frac{1}{4\pi\|\boldsymbol{x}-\boldsymbol{y}\|} \quad \text{for } d=3\,.$$

Existence and uniqueness of the solution of (2.1) follows from the $H^{-\frac{1}{2}}(\partial\Omega)$-ellipticity of a_V [28, Thm. 3.5.3], ensured after a suitable rescaling for $d = 2$.

2.2. **Boundary-Element Galerkin Discretization**

We introduce a mesh partition $\partial\Omega_h$ of $\partial\Omega$ whose cells are curve segments ($d = 2$) or curved triangular panels ($d = 3$). We perform a Galerkin discretization of (2.1) employing so-called boundary element spaces $\mathcal{S}_q^{-1}(\partial\Omega_h)$ of $\partial\Omega_h$-piecewise (mapped) polynomial functions of degree $q \in \mathbb{N}_0$. The simplest option $q = 0$ uses the boundary element space spanned by the characteristic functions of the cells of the mesh. For the details of the construction of $\mathcal{S}_q^{-1}(\partial\Omega_h)$ refer to [30, Ch. 10] or [28, Ch. 4]. The choice of basis functions and the computation of the Galerkin matrices is presented in [28, Ch. 5].

We restrict ourselves to the boundary element space $\mathcal{S}_0^{-1}(\partial\Omega_h)$ and write $\psi_h \in \mathcal{S}_0^{-1}(\partial\Omega_h)$ for the Galerkin boundary element solution of (2.1). The results of [28, §4.3] predict asymptotic convergence $\|\psi - \psi_h\|_{H^{-\frac{1}{2}}(\partial\Omega)} = O(h^{3/2})$ when the meshwidth h of $\partial\Omega_h$ is sent to zero through uniform regular refinement, and the exact solution ψ of (2.1) is sufficiently smooth.

2.3. **Surface Forces from BEM Solution**

With ψ_h at our disposal and in light of the fact that $\psi_h \approx \boldsymbol{\nabla} u \cdot \boldsymbol{n}|_{\partial\Omega}$ we can take the cue from (1.3) and try to approximate the surface force density $\mathbf{f}^\Gamma(\boldsymbol{x}) := \frac{1}{2}|\boldsymbol{\nabla} u(\boldsymbol{x})\cdot\boldsymbol{n}(\boldsymbol{x})|^2\boldsymbol{n}(\boldsymbol{x})$, $\boldsymbol{x} \in \Gamma$, by $\mathbf{f}_h^\Gamma(\boldsymbol{x}) := \frac{1}{2}|\psi_h(\boldsymbol{x})|^2\boldsymbol{n}(\boldsymbol{x})$. Thus we can compute an approximation of the total force as

$$\mathbf{F}_h := \int_\Gamma \mathbf{f}_h^\Gamma(\boldsymbol{x})\,\mathrm{d}S(\boldsymbol{x}) = \frac{1}{2}\int_\Gamma |\psi_h(\boldsymbol{x})|^2\boldsymbol{n}(\boldsymbol{x})\,\mathrm{d}S(\boldsymbol{x})\,. \tag{2.3}$$

However, this expression fails to be continuous on the trace space $H^{-\frac{1}{2}}(\partial\Omega)$ on which the variational BIE (2.1) is posed, as we only have the embedding $L^2(\partial\Omega) \subset H^{-\frac{1}{2}}(\partial\Omega)$ and the norm of $L^2(\partial\Omega)$ is strictly stronger than that of $H^{-\frac{1}{2}}(\partial\Omega)$.

Thus, Proposition 1.2 cannot be applied and we cannot expect that (2.3) will enjoy the superior accuracy and superconvergence gained by plugging Galerkin boundary element solutions into a twice continuously differentiable functional on $H^{-\frac{1}{2}}(\partial\Omega)$.

Experiment 2. We tackle the computation of total force for the 2D test cases of Experiment 1. We evaluate (2.3) for $\mathcal{S}_0^{-1}(\partial\Omega_h)$ boundary-element Galerkin solutions on quasi-uniform sequences of mesh partitions $\partial\Omega_h$ of $\partial\Omega$ with increasing resolution. An exact parametric representation of curved boundary parts was employed along with polar-coordinate transformation techniques for singular integrals [14, §9.4.5]. We add the resulting error curves to the plots of Experiment 1, see Figure 2.1.

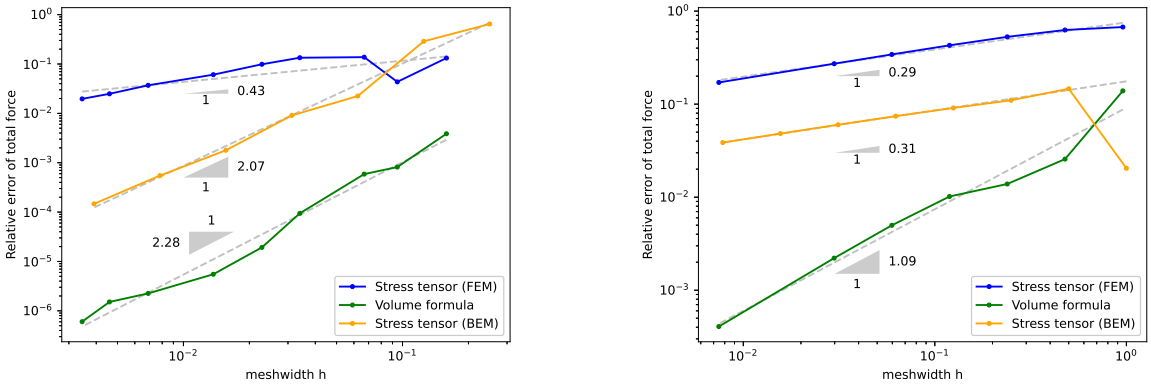

(A) Kite-shaped D

(B) Square-shaped D

FIGURE 2.1. Error of $\mathcal{S}_0^{-1}(\partial\Omega_h)$-BEM based forces by (2.3) ("Stress tensor (BEM)") as a function of the meshwidth h of $\partial\Omega_h$. Dashed lines represent the linear regression fits.

For the non-smooth square-shaped object we observe that both accuracy and convergence of the forces obtained from (2.3) are as poor as those for the boundary-based formula discussed in Section 1.2. Yet, for the kite-shaped smooth object, (2.3) delivers remarkable accuracy almost on par with that of volume-based formula used with the FEM.

In Experiment 1 volume-based force formula offered an attractive alternative to its boundary-based counterpart. Yet, the possibility to dispense with meshing Ω is a major advantage of boundary element methods that must not be sacrificed. Switching to volume-based formulas is not feasible in a BEM context. Hence, we need a Γ-based approach that is better behaved than (2.3).

3. Forces through Shape Differentiation

3.1. Virtual Work Principle

By the virtual work principle [17, 6, 4, 16, 3] in stationary settings force can be recovered as a shape derivative of the total co-energy $\mathcal{E} = \mathcal{E}(\Omega)$, which, for the linear electrostatic setting presented in Section 1.1, is the sum of the energy of the electric field in Ω

$$\mathcal{E}_F(\Omega) := \frac{1}{2}\int_\Omega \|\boldsymbol{\nabla} u(\boldsymbol{x})\|^2 \,\mathrm{d}\boldsymbol{x} = \frac{1}{2}\int_\Gamma g(\boldsymbol{x})\boldsymbol{\nabla} u(\boldsymbol{x})\cdot\boldsymbol{n}(\boldsymbol{x})\,\mathrm{d}S(\boldsymbol{x})\,, \tag{3.1}$$

where $u = u(\Omega)$ is the solution of (1.1), and of the energy $\mathcal{E}_B$ stored in the voltage source: $\mathcal{E} = \mathcal{E}_F + \mathcal{E}_B$.

Above we have indicated the dependence of both the electrostatic potential u and of the field energy $\mathcal{E}_F$ on the field domain Ω; both are "functions of the shape Ω". Of course, this entails specifying Dirichlet data $g \in H^{\frac{1}{2}}(\Gamma)$ for families of boundaries. We do this by regarding g as the restriction of a given

$\widetilde{g} \in H^1_0(B)$ to Γ: $g := \widetilde{g}|_\Gamma$. Of course, for the practical situation $g \equiv U$ we choose $\widetilde{g}$ to be constant in a neighborhood of Γ.

Next, we use the tools of shape calculus, in particular the so-called perturbation approach [29, §2.8], to give a rigorous meaning to what it means to "differentiate $\Omega \mapsto \mathcal{E}_F(\Omega)$" with respect to Ω. We start with the directional, Gateaux-type shape derivative with respect to a fixed smooth deformation vector field $\boldsymbol{\mathcal{V}} \in \left(C^\infty_0(B)\right)^d$ compactly supported in the hold-all domain B. It spawns the one-parameter family of perturbation maps

$$\mathsf{T}^t_{\boldsymbol{\mathcal{V}}} : B \to \mathbb{R}^d \,, \quad \mathsf{T}^t_{\boldsymbol{\mathcal{V}}}(\boldsymbol{x}) := \boldsymbol{x} + t\boldsymbol{\mathcal{V}}(\boldsymbol{x}) \,, \quad t \in \mathbb{R} \,, \tag{3.2}$$

The implicit function theorem ensures that there is $\delta = \delta(\boldsymbol{\mathcal{V}}) > 0$ such that $\mathsf{T}^t_{\boldsymbol{\mathcal{V}}}$ is a C^∞-diffeomorphism, if $|t| < \delta(\boldsymbol{\mathcal{V}})$. Therefore, all the deformed domains

$$\Omega_t := \mathsf{T}^t_{\boldsymbol{\mathcal{V}}}(\Omega) \,, \quad |t| < \delta(\boldsymbol{\mathcal{V}}) \,, \tag{3.3}$$

will still possess Lipschitz boundaries and all interfaces $\Gamma_t := \mathsf{T}^t_{\boldsymbol{\mathcal{V}}}(\Gamma)$ will be connected. Note that $\Omega_0 = \Omega$ and $\Gamma_0 = \Gamma$.

Then we call the limit

$$\frac{\mathrm{d}\mathcal{E}_F}{\mathrm{d}\Omega}(\Omega;\boldsymbol{\mathcal{V}}) := \lim_{t\to 0} \frac{\mathcal{E}_F(\Omega_t) - \mathcal{E}_F(\Omega)}{t} = \frac{\mathrm{d}}{\mathrm{d}t}\{t \mapsto \mathcal{E}_F(\Omega_t)\}\Big|_{t=0} \,, \tag{3.4}$$

if it exists, the shape (Gateaux) derivative of $\mathcal{E}_F$ at Ω in the direction of $\boldsymbol{\mathcal{V}}$. If, in addition, $\boldsymbol{\mathcal{V}} \mapsto \frac{\mathrm{d}\mathcal{E}_F}{\mathrm{d}\Omega}(\Omega;\boldsymbol{\mathcal{V}}) \in \mathbb{R}$ is a distribution on $\left(C^\infty_0(B)\right)^d$, a 1-current in the parlance of de Rham [8, Ch. 3, §8], then $\Omega \mapsto \mathcal{E}_F(\Omega)$ is called *shape-differentiable* and that distribution is the *shape derivative* $\frac{\mathrm{d}\mathcal{E}_F}{\mathrm{d}\Omega}(\Omega)$ of $\mathcal{E}_F$ in Ω. It is also our notion of *force field* for the electrostatic setting:

$$\text{force field} \quad \hat{=} \quad \text{The negative shape derivative,} \quad -\frac{\mathrm{d}\mathcal{E}_F}{\mathrm{d}\Omega}(\Omega), \quad \text{of the field energy } \mathcal{E}_F$$

Remark 3.1. What about the energy supplied by the voltage source, which sustains a constant voltage U? The change $\mathcal{E}^\Delta_B$ of the energy stored by the voltage source when deforming $\Omega = \Omega_0$ into Ω_t, $|t| < \delta$, is

$$\mathcal{E}^\Delta_B = -U(Q_t - Q_0) \quad \text{with charge} \quad Q_t := \int_{\Gamma_t} \boldsymbol{\nabla} u(\Omega_t;\boldsymbol{x}) \cdot \boldsymbol{n}(\boldsymbol{x}) \,\mathrm{d}S(\boldsymbol{x}) \,, \tag{3.5}$$

where $u = u(\Omega_t)$ is the solution of (1.1) with $g \equiv U$ on Γ_t. From (3.1) we immediately see that $\mathcal{E}^\Delta_B = -2\mathcal{E}^\Delta_F$, which means $\frac{\mathrm{d}\mathcal{E}}{\mathrm{d}\Omega}(\Omega) = -\frac{\mathrm{d}\mathcal{E}_F}{\mathrm{d}\Omega}(\Omega)$. This motivates the above definition of the force field, and in the sequel we focus on $\mathcal{E}_F$.

Remark 3.2. The Hadamard structure theorem [9, Ch. 9, Thm. 3.6] states that if Γ is C^∞-smooth, the shape derivative $\boldsymbol{\mathcal{V}} \mapsto \frac{\mathrm{d}\mathcal{E}_F}{\mathrm{d}\Omega}(\Omega;\boldsymbol{\mathcal{V}})$ admits a representative h in the space of distributions on $C^\infty(\Gamma)$

$$\frac{\mathrm{d}\mathcal{E}_F}{\mathrm{d}\Omega}(\Omega;\boldsymbol{\mathcal{V}}) = \langle h,\ \boldsymbol{\mathcal{V}} \cdot \boldsymbol{n}|_\Gamma \rangle \,, \quad \boldsymbol{\mathcal{V}} \in \left(C^\infty_0(B)\right)^d . \tag{3.6}$$

This distribution h can be regarded as representing a *normal surface force density.*

Remark 3.3. The Cartesian components of the *total force* $\mathbf{F} = (F_1, \ldots, F_d) \in \mathbb{R}^d$ acting on D are the shape derivatives with respect to deformation fields that agree with Cartesian coordinate vectors in a neighborhood of Γ:

$$F_k = -\frac{\mathrm{d}\mathcal{E}_F}{\mathrm{d}\Omega}(\Omega;\{\boldsymbol{x} \mapsto \mathbf{e}_k \chi(\boldsymbol{x})\}) \,, \tag{3.7}$$

where $\chi \in C^\infty_0(B)$, $\chi \equiv 1$ close to Γ.

The *total torque* T experienced by D with respect to the pivot point $\boldsymbol{c} \in B$ (and axis $\boldsymbol{a} \in \mathbb{R}^3$, $\|\boldsymbol{a}\| = 1$, for $d = 3$) is given by

$$T = \begin{cases} -\frac{\mathrm{d}\mathcal{E}_F}{\mathrm{d}\Omega}(\Omega, \{\boldsymbol{x} \mapsto (\boldsymbol{x} - \boldsymbol{c})^\perp\}) & \text{for} \quad d = 2\,, \\ -\frac{\mathrm{d}\mathcal{E}_F}{\mathrm{d}\Omega}(\Omega, \{\boldsymbol{x} \mapsto \boldsymbol{a} \times (\boldsymbol{x} - \boldsymbol{c})\}) & \text{for} \quad d = 3\,, \end{cases} \tag{3.8}$$

with $\perp$ indicating a plane rotation by $\pi/2$ and $\times$ denoting the vector product.

3.2. **Forces from Volume Variational Formulations**

The derivation of formulas for the directional shape derivative $\frac{\mathrm{d}\mathcal{E}_F}{\mathrm{d}\Omega}(\Omega; \boldsymbol{\mathcal{V}})$ is well established for the standard variational formulation (1.6) of (1.1), see [20, 9, 29]. With details postponed to Appendix A, we remark that "implicit shape differentiation" of (1.6) yields the boundary-based formula

$$\frac{\mathrm{d}\mathcal{E}_F}{\mathrm{d}\Omega}(\Omega; \boldsymbol{\mathcal{V}}) = \frac{1}{2} \int_\Gamma \left(((\boldsymbol{\nabla}\widetilde{g} - \boldsymbol{\nabla}u) \cdot \boldsymbol{n})(\boldsymbol{\nabla}u \cdot \boldsymbol{n}) + \boldsymbol{\nabla}\widetilde{g} \cdot \boldsymbol{\nabla}u \right) (\boldsymbol{\mathcal{V}} \cdot \boldsymbol{n}) \, \mathrm{d}S\,, \tag{3.9}$$

where u is the solution of (1.1), and $\boldsymbol{\mathcal{V}} \in \left(C_0^\infty(B)\right)^d$. Obviously, extra smoothness of u and $\widetilde{g}$ beyond merely $u \in H^1(\Omega)$ and $\widetilde{g} \in H_0^1(B)$ is required to render (3.9) meaningful. For $\widetilde{g} \equiv U$ and $\boldsymbol{\mathcal{V}}$ constant in a neighborhood of Γ we recover the classical formula (1.3).

In fact, also the volume-based force formula (1.4) can be obtained as a shape derivative. Again, we start from the standard variational formulation on Ω_t:

$$u = u(\Omega_t) \in H_0^1(\Omega_t) + \widetilde{g}: \quad \int_{\Omega_t} \boldsymbol{\nabla}u(\boldsymbol{x}) \cdot \boldsymbol{\nabla}v(\boldsymbol{x}) \, \mathrm{d}\boldsymbol{x} = 0 \quad \forall v \in H_0^1(\Omega_t)\,, \tag{3.10}$$

and then pull it back to $\Omega = \Omega_0$. We arrive at a variational characterization of the pullback $\widehat{u}(t) := u(\Omega_t) \circ \mathsf{T}_{\boldsymbol{\mathcal{V}}}^t$: Seek $\widehat{u} = \widehat{u}(t) \in H_0^1(\Omega) + \widetilde{g} \circ \mathsf{T}_{\boldsymbol{\mathcal{V}}}^t$ such that

$$\int_\Omega \left((\mathsf{D}\mathsf{T}_{\boldsymbol{\mathcal{V}}}^t(\widehat{\boldsymbol{x}}))^{-1} (\mathsf{D}\mathsf{T}_{\boldsymbol{\mathcal{V}}}^t(\widehat{\boldsymbol{x}}))^{-\top} \boldsymbol{\nabla}\widehat{u}(\widehat{\boldsymbol{x}}) \right) \cdot \boldsymbol{\nabla}v(\widehat{\boldsymbol{x}}) \, |\det \mathsf{D}\mathsf{T}_{\boldsymbol{\mathcal{V}}}^t(\widehat{\boldsymbol{x}})| \, \mathrm{d}\widehat{\boldsymbol{x}} = 0 \tag{3.11}$$

for all $v \in H_0^1(\Omega)$. This confines the t-dependence to the integrand. The same trick works for the field energy

$$\mathcal{E}_F(t) := \int_\Omega \|(\mathsf{D}\mathsf{T}_{\boldsymbol{\mathcal{V}}}^t(\widehat{\boldsymbol{x}}))^{-\top} \boldsymbol{\nabla}\widehat{u}(t)(\widehat{\boldsymbol{x}})\|^2 |\det \mathsf{D}\mathsf{T}_{\boldsymbol{\mathcal{V}}}^t(\widehat{\boldsymbol{x}})| \, \mathrm{d}\widehat{\boldsymbol{x}}\,. \tag{3.12}$$

Then computing the shape derivative $\frac{\mathrm{d}\mathcal{E}_F}{\mathrm{d}\Omega}(\Omega; \boldsymbol{\mathcal{V}}) = \frac{\mathrm{d}\mathcal{E}_F}{\mathrm{d}t}(0)$ using the adjoint approach from PDE-constraint optimization, see Appendix B, yields a volume-based formula, which boils down to (1.4) for $\widetilde{g} \equiv U$ in a neighborhood of Γ and suitably chosen $\boldsymbol{\mathcal{V}}$.

4. **BIE-Based Shape Derivative of Field Energy**

4.1. **Pullback of BIEs**

In Section 3.2, see also Appendix B, we learned that via the pullback approach to shape differentiation we obtain volume-based expressions that are smooth functionals on $H^1(\Omega)$, the function space framework for the standard variational formulation. The gist of the pullback approach is to avoid t-dependent domains of integration Ω_t by mapping to the fixed domain Ω.

Now we pursue this policy for the variational boundary integral equation (2.1). As in (3.3) we write $\left(\Omega_t := \mathsf{T}_{\boldsymbol{\mathcal{V}}}^t(\Omega)\right)_{|t|<\delta}$ for the 1-parameter family of slightly deformed domains induced by a given deformation vector field $\boldsymbol{\mathcal{V}} \in \left(C_0^\infty(B)\right)^d$. Replacing $\partial\Omega \to \partial\Omega_t$ and $\Gamma \to \Gamma_t := \mathsf{T}_{\boldsymbol{\mathcal{V}}}^t(\Gamma)$ in the formulas (2.2)

yields a t-dependent version of (2.1): for $t \in]-\delta,\delta[$

$$\psi(t) \in H^{-\frac{1}{2}}(\partial\Omega_t): \quad \mathsf{a}_V(t;\psi(t),\varphi) = \frac{1}{2}\ell_g(t;\varphi) + \mathsf{b}_K(t;g,\varphi) \quad \forall \varphi \in H^{-\frac{1}{2}}(\partial\Omega_t)\,. \tag{4.1}$$

In these formulas, $g \in H^{\frac{1}{2}}(\partial\Omega_t)$ should be understood as the trace $\widetilde{g}|_{\Gamma_t}$ of a $\widetilde{g} \in H^1_0(B)$. The field energy as given in (3.1) also becomes a function of t:

$$\mathcal{E}_F(t) = J(t;\psi(t))\,, \quad J(t;\varphi) := \frac{1}{2}\int_{\Gamma_t} \varphi(\boldsymbol{x})\widetilde{g}(\boldsymbol{x})\,\mathrm{d}S(\boldsymbol{x})\,, \quad \varphi \in H^{-\frac{1}{2}}(\Gamma_t)\,. \tag{4.2}$$

The surface integrals can be transformed to $\partial\Omega$ using the following identity [9, Ch. 9, §4.2, eq. 4.9], [29, §2.17]:

$$\int_{\partial\Omega_t} f(\boldsymbol{x})\,\mathrm{d}S(\boldsymbol{x}) = \int_{\partial\Omega} f(\mathsf{T}^t_{\boldsymbol{\mathcal{V}}}(\widehat{\boldsymbol{x}}))\,\omega_t(\widehat{\boldsymbol{x}})\,\mathrm{d}S(\widehat{\boldsymbol{x}}), \quad \omega_t(\widehat{\boldsymbol{x}}) = \|\mathbf{C}(\mathsf{D}\mathsf{T}^t_{\boldsymbol{\mathcal{V}}}(\widehat{\boldsymbol{x}}))\,\boldsymbol{n}(\widehat{\boldsymbol{x}})\|\,, \tag{4.3}$$

where $\mathbf{C}(\mathbf{M})$ denotes the co-factor matrix for $\mathbf{M} \in \mathbb{R}^{d,d}$. We also need a transformation rule for the unit normal vector field $\boldsymbol{n}_t$ on $\partial\Omega_t$ [9, Ch. 9, Thm. 4.4]:

$$\boldsymbol{n}_t(\boldsymbol{x}) = \frac{\mathbf{C}(\mathsf{D}\mathsf{T}^t_{\boldsymbol{\mathcal{V}}}(\widehat{\boldsymbol{x}}))\,\boldsymbol{n}(\widehat{\boldsymbol{x}})}{\|\mathbf{C}(\mathsf{D}\mathsf{T}^t_{\boldsymbol{\mathcal{V}}}(\widehat{\boldsymbol{x}}))\,\boldsymbol{n}(\widehat{\boldsymbol{x}})\|} = \frac{\mathbf{C}(\mathsf{D}\mathsf{T}^t_{\boldsymbol{\mathcal{V}}}(\widehat{\boldsymbol{x}}))\,\boldsymbol{n}(\widehat{\boldsymbol{x}})}{\omega_t(\widehat{\boldsymbol{x}})}\,, \quad \boldsymbol{x} := \mathsf{T}^t_{\boldsymbol{\mathcal{V}}}(\widehat{\boldsymbol{x}}),\ \widehat{\boldsymbol{x}} \in \partial\Omega\,. \tag{4.4}$$

Using these transformation rules the building blocks of (4.1) can be written by means of integrals over $\partial\Omega$:

$$\begin{aligned}
\mathsf{a}_V(t;\psi,\varphi) &= \int_{\partial\Omega}\int_{\partial\Omega} G(\mathsf{T}^t_{\boldsymbol{\mathcal{V}}}(\widehat{\boldsymbol{x}}),\mathsf{T}^t_{\boldsymbol{\mathcal{V}}}(\widehat{\boldsymbol{y}}))\,\psi(\mathsf{T}^t_{\boldsymbol{\mathcal{V}}}(\widehat{\boldsymbol{y}}))\,\varphi(\mathsf{T}^t_{\boldsymbol{\mathcal{V}}}(\widehat{\boldsymbol{x}}))\,\omega_t(\widehat{\boldsymbol{y}})\,\omega_t(\widehat{\boldsymbol{x}})\,\mathrm{d}S(\widehat{\boldsymbol{y}})\mathrm{d}S(\widehat{\boldsymbol{x}})\,,\\
\mathsf{b}_K(t;g,\varphi) &= \int_{\partial\Omega}\int_{\partial\Omega} \Big\{\boldsymbol{\nabla}_{\boldsymbol{y}} G(\mathsf{T}^t_{\boldsymbol{\mathcal{V}}}(\widehat{\boldsymbol{x}}),\mathsf{T}^t_{\boldsymbol{\mathcal{V}}}(\widehat{\boldsymbol{y}}))\cdot\mathbf{C}(\mathsf{D}\mathsf{T}^t_{\boldsymbol{\mathcal{V}}}(\widehat{\boldsymbol{y}}))\boldsymbol{n}(\widehat{\boldsymbol{y}})\Big\}\\
&\qquad\qquad \cdot g(\mathsf{T}^t_{\boldsymbol{\mathcal{V}}}(\widehat{\boldsymbol{y}}))\,\varphi(\mathsf{T}^t_{\boldsymbol{\mathcal{V}}}(\widehat{\boldsymbol{x}}))\,\omega_t(\widehat{\boldsymbol{x}})\,\mathrm{d}S(\widehat{\boldsymbol{y}})\mathrm{d}S(\widehat{\boldsymbol{x}})\,,\\
\ell_g(t;\varphi) &= \int_{\partial\Omega} g(\mathsf{T}^t_{\boldsymbol{\mathcal{V}}}(\widehat{\boldsymbol{x}}))\,\varphi(\mathsf{T}^t_{\boldsymbol{\mathcal{V}}}(\widehat{\boldsymbol{x}}))\,\omega_t(\widehat{\boldsymbol{x}})\,\mathrm{d}S(\widehat{\boldsymbol{x}})\,,
\end{aligned}$$

and the expression for the energy becomes

$$J(t;\psi) = \frac{1}{2}\int_{\Gamma} \psi(\mathsf{T}^t_{\boldsymbol{\mathcal{V}}}(\widehat{\boldsymbol{x}}))\,g(\mathsf{T}^t_{\boldsymbol{\mathcal{V}}}(\widehat{\boldsymbol{x}}))\,\omega_t(\widehat{\boldsymbol{x}})\,\mathrm{d}S(\widehat{\boldsymbol{x}})\,.$$

Since the nature of $\psi(t)$ is that of a surface charge density, we pull back $\psi(t)$ to the space $H^{-\frac{1}{2}}(\partial\Omega)$ using the pullback of surface densities, which is generically defined as

$$\widehat{\varphi}(\widehat{\boldsymbol{x}}) := \varphi(\mathsf{T}^t_{\boldsymbol{\mathcal{V}}}(\widehat{\boldsymbol{x}}))\,\omega_t(\widehat{\boldsymbol{x}})\,, \quad \widehat{\boldsymbol{x}} \in \partial\Omega\,, \quad \varphi \in H^{-\frac{1}{2}}(\partial\Omega_t)\,. \tag{4.5}$$

Thus, we find that $\widehat{\psi}(t)$ satisfies the transformed variational boundary integral equation

$$\widehat{\psi}(t) \in H^{-\frac{1}{2}}(\partial\Omega): \quad \widehat{\mathsf{a}}_V(t;\widehat{\psi},\widehat{\varphi}) = \frac{1}{2}\widehat{\ell}_{\widetilde{g}}(t;\widehat{\varphi}) + \widehat{\mathsf{b}}_K(t;\widetilde{g},\varphi) \quad \forall \widehat{\varphi} \in H^{-\frac{1}{2}}(\partial\Omega)\,, \tag{4.6}$$

with the abbreviations ($\widehat{\sigma},\widehat{\varphi} \in H^{-\frac{1}{2}}(\partial\Omega)$)

$$\widehat{\mathsf{a}}_V(t;\widehat{\sigma},\widehat{\varphi}) := \int_{\partial\Omega}\int_{\partial\Omega} G(\mathsf{T}^t_{\boldsymbol{\mathcal{V}}}(\widehat{\boldsymbol{x}}),\mathsf{T}^t_{\boldsymbol{\mathcal{V}}}(\widehat{\boldsymbol{y}}))\,\widehat{\sigma}(\widehat{\boldsymbol{y}})\,\widehat{\varphi}(\widehat{\boldsymbol{x}})\,\mathrm{d}S(\widehat{\boldsymbol{y}})\mathrm{d}S(\widehat{\boldsymbol{x}})\,, \tag{4.7a}$$

$$\begin{aligned}
\widehat{\mathsf{b}}_K(t;\widetilde{g},\widehat{\varphi}) := \int_{\partial\Omega}\int_{\partial\Omega} &\Big\{\boldsymbol{\nabla}_{\boldsymbol{y}} G(\mathsf{T}^t_{\boldsymbol{\mathcal{V}}}(\widehat{\boldsymbol{x}}),\mathsf{T}^t_{\boldsymbol{\mathcal{V}}}(\widehat{\boldsymbol{y}}))\cdot\mathbf{C}(\mathsf{D}\mathsf{T}^t_{\boldsymbol{\mathcal{V}}}(\widehat{\boldsymbol{y}}))\boldsymbol{n}(\widehat{\boldsymbol{y}})\Big\}\\
&\cdot \widetilde{g}(\mathsf{T}^t_{\boldsymbol{\mathcal{V}}}(\widehat{\boldsymbol{y}}))\,\widehat{\varphi}(\widehat{\boldsymbol{x}})\,\mathrm{d}S(\widehat{\boldsymbol{y}})\mathrm{d}S(\widehat{\boldsymbol{x}})\,,
\end{aligned} \tag{4.7b}$$

$$\widehat{\ell}_{\widetilde{g}}(t;\widehat{\varphi}) := \int_{\partial\Omega} \widetilde{g}(\mathsf{T}^t_{\boldsymbol{\mathcal{V}}}(\widehat{\boldsymbol{x}}))\,\widehat{\varphi}(\widehat{\boldsymbol{x}})\,\mathrm{d}S(\widehat{\boldsymbol{x}})\,. \tag{4.7c}$$

The transformed expression for the energy turns out as

$$\widehat{\mathcal{E}}_F(\boldsymbol{\mathcal{V}};t) := \widehat{J}(t;\widehat{\psi}(t)) \;, \quad \widehat{J}(t;\widehat{\varphi}) := \frac{1}{2}\int_\Gamma \widehat{\varphi}(\widehat{\boldsymbol{x}})\, \widetilde{g}(\mathsf{T}^t_{\boldsymbol{\mathcal{V}}}(\widehat{\boldsymbol{x}}))\, \mathrm{d}S(\widehat{\boldsymbol{x}}) \;. \tag{4.8}$$

4.2. **BIE-Constrained Shape Derivative**

In order to compute the shape derivative $\frac{\mathrm{d}\mathcal{E}_F}{\mathrm{d}\Omega}(\Omega;\boldsymbol{\mathcal{V}}) = \frac{\mathrm{d}\widehat{\mathcal{E}}_F}{\mathrm{d}t}(\boldsymbol{\mathcal{V}};0)$ for $t \mapsto \widehat{\mathcal{E}}_F(\boldsymbol{\mathcal{V}};t)$ from (4.8) with $t \mapsto \widehat{\psi}(t)$ defined through the linear variational equation (4.6) we resort to the well-established adjoint approach [19, §1.6.4]. The relevant Lagrangian is given by

$$L(t;\widehat{\sigma},\widehat{\varphi}) := \widehat{J}(t;\widehat{\sigma}) + \widehat{\mathsf{a}}_V(t;\widehat{\sigma},\widehat{\varphi}) - \frac{1}{2}\widehat{\ell}_{\widetilde{g}}(t;\widehat{\varphi}) - \widehat{\mathsf{b}}_K(t;\widetilde{g},\widehat{\varphi}) \;, \quad \widehat{\sigma},\widehat{\varphi} \in H^{-\frac{1}{2}}(\partial\Omega) \;, \tag{4.9}$$

and, writing $\widehat{\psi}(t)$ for the solution of (4.6), it permits us to express $\widehat{\mathcal{E}}_F(\boldsymbol{\mathcal{V}};t)$ as

$$\widehat{\mathcal{E}}_F(\boldsymbol{\mathcal{V}};t) = \widehat{J}(t;\widehat{\psi}(t)) = L(t;\widehat{\psi}(t),\widehat{\varphi}) \quad \forall \widehat{\varphi} \in H^{-\frac{1}{2}}(\partial\Omega) \;. \tag{4.10}$$

We exploit the freedom of being able to insert any $\widehat{\varphi} \in H^{-\frac{1}{2}}(\partial\Omega)$ into (4.10) and choose it as the solution ρ of the *adjoint variational problem*: seek $\rho \in H^{-\frac{1}{2}}(\partial\Omega)$ such that

$$\begin{aligned} & \widehat{\mathsf{a}}_V(0;\widehat{\varphi},\rho) = -\left\langle \frac{\partial \widehat{J}}{\partial \widehat{\psi}}(0;\widehat{\psi}(0)),\widehat{\varphi}\right\rangle \quad \forall \widehat{\varphi} \in H^{-\frac{1}{2}}(\partial\Omega) \\ \iff \qquad & \mathsf{a}_V(\varphi,\rho) = -\frac{1}{2}\int_\Gamma \varphi(\widehat{\boldsymbol{x}})\, g(\widehat{\boldsymbol{x}})\, \mathrm{d}S(\widehat{\boldsymbol{x}}) \quad \forall \varphi \in H^{-\frac{1}{2}}(\partial\Omega) \;. \end{aligned} \tag{4.11}$$

Noting that $\widehat{\psi}(0) = \psi$, ψ the solution of the BIE (2.1), this yields the formula

$$\frac{\mathrm{d}\widehat{\mathcal{E}}_F}{\mathrm{d}t}(\boldsymbol{\mathcal{V}};0) = \frac{\partial L}{\partial t}(0;\widehat{\psi}(0),\rho) = \frac{\partial \widehat{J}}{\partial t}(0;\psi) + \frac{\partial \widehat{\mathsf{a}}_V}{\partial t}(0;\psi,\rho) - \frac{1}{2}\frac{\partial \widehat{\ell}_{\widetilde{g}}}{\partial t}(0;\rho) - \frac{\widehat{\mathsf{b}}_K}{\partial t}(0;\widetilde{g},\rho) \;. \tag{4.12}$$

It expresses the directional shape derivative of $\widehat{\mathcal{E}}_F$ by means of partial derivatives with respect to t of the terms in (4.6). Those partial derivatives can be computed using the definition of $\mathsf{T}^t_{\boldsymbol{\mathcal{V}}}$ and the formulas [29, §2.13]

$$\left.\frac{\mathrm{d}(\mathsf{D}\mathsf{T}^t_{\boldsymbol{\mathcal{V}}})}{\mathrm{d}t}\right|_{t=0} = \mathsf{D}\boldsymbol{\mathcal{V}} \;, \quad \left.\frac{\mathrm{d}\det(\mathsf{D}\mathsf{T}^t_{\boldsymbol{\mathcal{V}}})}{\mathrm{d}t}\right|_{t=0} = \boldsymbol{\nabla}\cdot\boldsymbol{\mathcal{V}} \;, \quad \left.\frac{\mathrm{d}(f\circ\mathsf{T}^t_{\boldsymbol{\mathcal{V}}})}{\mathrm{d}t}\right|_{t=0} = \boldsymbol{\nabla} f\cdot\boldsymbol{\mathcal{V}} \;, \tag{4.13}$$

along with the expressions

$$\left.\frac{\mathrm{d}(\mathsf{D}\mathsf{T}^t_{\boldsymbol{\mathcal{V}}})^{-1}}{\mathrm{d}t}\right|_{t=0} = \; -\left(\mathsf{D}\mathsf{T}^t_{\boldsymbol{\mathcal{V}}}\right)^{-1}\frac{\mathrm{d}\,\mathsf{D}\mathsf{T}^t_{\boldsymbol{\mathcal{V}}}}{\mathrm{d}t}\left(\mathsf{D}\mathsf{T}^t_{\boldsymbol{\mathcal{V}}}\right)^{-1}\Big|_{t=0} = -\mathbf{I}_d\,\mathsf{D}\boldsymbol{\mathcal{V}}\,\mathbf{I}_d = -\mathsf{D}\boldsymbol{\mathcal{V}} \;, \tag{4.14}$$

$$\left.\frac{\mathrm{d}\mathbf{C}(\mathsf{D}\mathsf{T}^t_{\boldsymbol{\mathcal{V}}})}{\mathrm{d}t}\right|_{t=0} = \left.\frac{\mathrm{d}\left(\det\mathsf{D}\mathsf{T}^t_{\boldsymbol{\mathcal{V}}}\,\left(\mathsf{D}\mathsf{T}^t_{\boldsymbol{\mathcal{V}}}\right)^{-\top}\right)}{\mathrm{d}t}\right|_{t=0} = (\boldsymbol{\nabla}\cdot\boldsymbol{\mathcal{V}})\,\mathbf{I}_d - (\mathsf{D}\boldsymbol{\mathcal{V}})^\top \;, \tag{4.15}$$

$$\left.\frac{\mathrm{d}\omega_t}{\mathrm{d}t}\right|_{t=0} = \left.\frac{\mathrm{d}\|\mathbf{C}(\mathsf{D}\mathsf{T}^t_{\boldsymbol{\mathcal{V}}})\boldsymbol{n}\|}{\mathrm{d}t}\right|_{t=0} = \boldsymbol{n}\cdot(\boldsymbol{\nabla}\cdot\boldsymbol{\mathcal{V}}\,\boldsymbol{n} - (\mathsf{D}\boldsymbol{\mathcal{V}})^\top\boldsymbol{n}) = \boldsymbol{\nabla}\cdot\boldsymbol{\mathcal{V}} - \boldsymbol{n}\cdot(\mathsf{D}\boldsymbol{\mathcal{V}})^\top\boldsymbol{n} \;. \tag{4.16}$$

Thus, swapping differentiation and integration in (4.7) we get

$$
\begin{aligned}
\frac{\partial \widehat{\mathsf{a}}_V}{\partial t}(0;\psi,\rho) &= \int_{\partial\Omega}\int_{\partial\Omega} \left.\frac{\mathrm{d}\, G(\mathsf{T}^t_{\boldsymbol{\mathcal{V}}}(\widehat{\boldsymbol{x}}),\mathsf{T}^t_{\boldsymbol{\mathcal{V}}}(\widehat{\boldsymbol{y}}))}{\mathrm{d}t}\right|_{t=0} \psi(\widehat{\boldsymbol{y}})\;\rho(\widehat{\boldsymbol{x}})\,\mathrm{d}S(\widehat{\boldsymbol{y}})\mathrm{d}S(\widehat{\boldsymbol{x}})\;,\\
&= \int_{\partial\Omega}\int_{\partial\Omega} \left(\boldsymbol{\nabla}_{\boldsymbol{x}} G(\widehat{\boldsymbol{x}},\widehat{\boldsymbol{y}})\cdot\boldsymbol{\mathcal{V}}(\widehat{\boldsymbol{x}}) + \boldsymbol{\nabla}_{\boldsymbol{y}} G(\widehat{\boldsymbol{x}},\widehat{\boldsymbol{y}})\cdot\boldsymbol{\mathcal{V}}(\widehat{\boldsymbol{y}})\right)\psi(\widehat{\boldsymbol{y}})\;\rho(\widehat{\boldsymbol{x}})\,\mathrm{d}S(\widehat{\boldsymbol{y}})\mathrm{d}S(\widehat{\boldsymbol{x}})\;.\\
\frac{\partial \widehat{\mathsf{b}}_K}{\partial t}(0;\widetilde{g},\rho) &= \int_{\partial\Omega}\int_{\partial\Omega} \rho(\widehat{\boldsymbol{x}})\left.\frac{\mathrm{d}((\boldsymbol{\nabla}_{\boldsymbol{y}} G(\mathsf{T}^t_{\boldsymbol{\mathcal{V}}}(\widehat{\boldsymbol{x}}),\mathsf{T}^t_{\boldsymbol{\mathcal{V}}}(\widehat{\boldsymbol{y}}))\cdot\mathbf{C}(\mathsf{D}\mathsf{T}^t_{\boldsymbol{\mathcal{V}}}(\widehat{\boldsymbol{y}}))\,\boldsymbol{n}(\widehat{\boldsymbol{y}}))\;\widetilde{g}(\mathsf{T}^t_{\boldsymbol{\mathcal{V}}}(\widehat{\boldsymbol{y}})))}{\mathrm{d}t}\right|_{t=0}\mathrm{d}S(\widehat{\boldsymbol{y}})\mathrm{d}S(\widehat{\boldsymbol{x}})\\
&= \int_{\partial\Omega}\int_{\partial\Omega} p(\widehat{\boldsymbol{x}})\,\widetilde{g}(\widehat{\boldsymbol{y}})\;\left.\frac{\mathrm{d}\boldsymbol{\nabla}_{\boldsymbol{y}} G(\mathsf{T}^t_{\boldsymbol{\mathcal{V}}}(\widehat{\boldsymbol{x}}),\mathsf{T}^t_{\boldsymbol{\mathcal{V}}}(\widehat{\boldsymbol{y}}))}{\mathrm{d}t}\right|_{t=0}\cdot\boldsymbol{n}(\widehat{\boldsymbol{y}})\,\mathrm{d}S(\widehat{\boldsymbol{y}})\mathrm{d}S(\widehat{\boldsymbol{x}})\\
&\quad+\int_{\partial\Omega}\int_{\partial\Omega} \rho(\widehat{\boldsymbol{x}})\,\widetilde{g}(\widehat{\boldsymbol{y}})\;\boldsymbol{\nabla}_{\boldsymbol{y}} G(\widehat{\boldsymbol{x}},\widehat{\boldsymbol{y}})\cdot(\boldsymbol{\nabla}\cdot\boldsymbol{\mathcal{V}}(\widehat{\boldsymbol{y}})\,\boldsymbol{n}(\widehat{\boldsymbol{y}}) - \mathsf{D}\boldsymbol{\mathcal{V}}^\top(\widehat{\boldsymbol{y}})\boldsymbol{n}(\widehat{\boldsymbol{y}}))\,\mathrm{d}S(\widehat{\boldsymbol{y}})\mathrm{d}S(\widehat{\boldsymbol{x}})\\
&\quad+\int_{\partial\Omega}\int_{\partial\Omega} \rho(\widehat{\boldsymbol{x}})(\boldsymbol{\nabla}_{\boldsymbol{y}} G(\widehat{\boldsymbol{x}},\widehat{\boldsymbol{y}})\cdot\boldsymbol{n}(\widehat{\boldsymbol{y}}))(\boldsymbol{\nabla}\widetilde{g}(\widehat{\boldsymbol{y}})\cdot\boldsymbol{\mathcal{V}}(\widehat{\boldsymbol{y}}))\,\mathrm{d}S(\widehat{\boldsymbol{y}})\mathrm{d}S(\widehat{\boldsymbol{x}})\;,\\
\frac{\partial \widehat{\ell}_{\widetilde{g}}}{\partial t}(0;\rho) &= \int_{\partial\Omega}\rho(\widehat{\boldsymbol{x}})\left.\frac{\mathrm{d}\,\widetilde{g}(\mathsf{T}^t_{\boldsymbol{\mathcal{V}}}(\widehat{\boldsymbol{x}}))}{\mathrm{d}t}\right|_{t=0}\mathrm{d}S(\boldsymbol{x}) = \int_{\partial\Omega}\rho(\widehat{\boldsymbol{x}})\boldsymbol{\nabla}\widetilde{g}(\widehat{\boldsymbol{x}})\cdot\boldsymbol{\mathcal{V}}(\widehat{\boldsymbol{x}})\,\mathrm{d}S(\widehat{\boldsymbol{x}})\;,\\
\frac{\partial \widehat{J}}{\partial t}(0;\psi) &= \frac{1}{2}\int_{\Gamma}\psi(\widehat{\boldsymbol{x}})\left.\frac{\mathrm{d}\,\widetilde{g}(T_t(\widehat{\boldsymbol{x}}))}{\mathrm{d}t}\right|_{t=0}\mathrm{d}S(\boldsymbol{x}) = \frac{1}{2}\int_{\Gamma}\psi(\widehat{\boldsymbol{x}})\boldsymbol{\nabla}\widetilde{g}(\widehat{\boldsymbol{x}})\cdot\boldsymbol{\mathcal{V}}(\widehat{\boldsymbol{x}})\,\mathrm{d}S(\widehat{\boldsymbol{x}})\;.
\end{aligned}
$$

Adding up individual contributions gives us the directional shape derivative

$$
\begin{aligned}
&\frac{\mathrm{d}\widehat{\mathcal{E}}_F}{\mathrm{d}t}(\boldsymbol{\mathcal{V}};0)\,[\psi,\rho]\\
&= \frac{1}{2}\int_{\Gamma}\psi(\widehat{\boldsymbol{x}})\;(\boldsymbol{\nabla}\widetilde{g}(\widehat{\boldsymbol{x}})\cdot\boldsymbol{\mathcal{V}}(\widehat{\boldsymbol{x}}))\,\mathrm{d}S(\widehat{\boldsymbol{x}}) && =:\mathbf{T_1}(\psi)\\
&\quad+\int_{\partial\Omega}\int_{\partial\Omega}\psi(\widehat{\boldsymbol{y}})\;\{\boldsymbol{\nabla}_{\boldsymbol{x}} G(\widehat{\boldsymbol{x}},\widehat{\boldsymbol{y}})\cdot\boldsymbol{\mathcal{V}}(\widehat{\boldsymbol{x}})+\boldsymbol{\nabla}_{\boldsymbol{y}} G(\widehat{\boldsymbol{x}},\widehat{\boldsymbol{y}})\cdot\boldsymbol{\mathcal{V}}(\widehat{\boldsymbol{y}})\}\;\rho(\widehat{\boldsymbol{x}})\,\mathrm{d}S(\widehat{\boldsymbol{y}})\mathrm{d}S(\widehat{\boldsymbol{x}}) && =:\mathbf{T_2}(\psi,\rho)\\
&\quad-\int_{\partial\Omega}\int_{\partial\Omega}\rho(\widehat{\boldsymbol{x}})\widetilde{g}(\widehat{\boldsymbol{y}})\;\left.\frac{\mathrm{d}\boldsymbol{\nabla}_{\boldsymbol{y}} G(\mathsf{T}^t_{\boldsymbol{\mathcal{V}}}(\widehat{\boldsymbol{x}}),\mathsf{T}^t_{\boldsymbol{\mathcal{V}}}(\widehat{\boldsymbol{y}}))}{\mathrm{d}t}\right|_{t=0}\cdot\boldsymbol{n}(\widehat{\boldsymbol{y}})\,\mathrm{d}S(\widehat{\boldsymbol{y}})\mathrm{d}S(\widehat{\boldsymbol{x}}) && =:\mathbf{T_3}(\rho) \qquad (4.17)\\
&\quad+\int_{\partial\Omega}\int_{\partial\Omega}\rho(\widehat{\boldsymbol{x}})\widetilde{g}(\widehat{\boldsymbol{y}})\;\boldsymbol{\nabla}_{\boldsymbol{y}} G(\widehat{\boldsymbol{x}},\widehat{\boldsymbol{y}})\cdot((\mathsf{D}\boldsymbol{\mathcal{V}})^\top(\widehat{\boldsymbol{y}})\boldsymbol{n}(\widehat{\boldsymbol{y}}))\,\mathrm{d}S(\widehat{\boldsymbol{y}})\mathrm{d}S(\widehat{\boldsymbol{x}}) && =:\mathbf{T_4}(\rho)\\
&\quad-\int_{\partial\Omega}\int_{\partial\Omega}\rho(\widehat{\boldsymbol{x}})(\boldsymbol{\nabla}_{\boldsymbol{y}} G(\widehat{\boldsymbol{x}},\widehat{\boldsymbol{y}})\cdot\widehat{\boldsymbol{n}}(\widehat{\boldsymbol{y}}))\boldsymbol{\nabla}\cdot(\widetilde{g}(\widehat{\boldsymbol{y}})\boldsymbol{\mathcal{V}}(\widehat{\boldsymbol{y}}))\,\mathrm{d}S(\widehat{\boldsymbol{y}})\mathrm{d}S(\widehat{\boldsymbol{x}}) && =:\mathbf{T_5}(\rho)\\
&\quad-\frac{1}{2}\int_{\partial\Omega}\rho(\widehat{\boldsymbol{x}})\;(\boldsymbol{\nabla}\widetilde{g}(\widehat{\boldsymbol{x}})\cdot\boldsymbol{\mathcal{V}}(\widehat{\boldsymbol{x}}))\,\mathrm{d}S(\widehat{\boldsymbol{x}})\;. && =:\mathbf{T_6}(\rho)
\end{aligned}
$$

The notation $\frac{\mathrm{d}\widehat{\mathcal{E}}_F}{\mathrm{d}t}(\boldsymbol{\mathcal{V}};0)\,[\psi,\rho]$ hints that this expression can be viewed as a function of the two arguments $\psi\in H^{-\frac{1}{2}}(\partial\Omega)$ and $\rho\in H^{-\frac{1}{2}}(\partial\Omega)$, for which we have to plug in the solutions of the "state problem" (2.1) and of the adjoint problem (4.11), respectively, in order to recover the force in direction $\boldsymbol{\mathcal{V}}$.

4.3. **BEM-Based Approximation of Forces**

To evaluate the shape derivative (4.17) for a displacement vector field $\boldsymbol{\mathcal{V}}$, beside the data $\widetilde{g}$ we need the solutions $\psi\in H^{-\frac{1}{2}}(\partial\Omega)$ (state solution) and $\rho\in H^{-\frac{1}{2}}(\partial\Omega)$ (adjoint solution) of the weakly singular variational boundary integral equations (2.1) and (4.11), respectively.

In general, those will only be available through boundary element Galerkin approximations as introduced in Section 2.2. In other words, we evaluate (4.17) after replacing ψ and ρ with Galerkin approximations ψ_h and ρ_h. This gives an approximation for the action of the surface force density on the displacement $\boldsymbol{\mathcal{V}}$, the "force in direction $\boldsymbol{\mathcal{V}}$",

$$\int_\Gamma \mathbf{f}^\Gamma(\boldsymbol{x}) \cdot \boldsymbol{\mathcal{V}}(\boldsymbol{x}) \,\mathrm{d}S(\boldsymbol{x}) \approx -\frac{\mathrm{d}\widehat{\mathcal{E}}_F}{\mathrm{d}t}(\boldsymbol{\mathcal{V}};0)\,[\psi_h,\rho_h] \ . \tag{4.18}$$

Neglecting potential variational crimes this perfectly fits the abstract framework of Section 1.3 and Proposition 1.2 with $V := H^{-\frac{1}{2}}(\partial\Omega) \times H^{-\frac{1}{2}}(\partial\Omega)$, $\mathsf{a} := \mathsf{a}_V \times \mathsf{a}_V$, and $F((\varphi,\sigma)) := \frac{\mathrm{d}\widehat{\mathcal{E}}_F}{\mathrm{d}t}(\boldsymbol{\mathcal{V}};0)\,[\varphi,\sigma]$.

Obviously the mapping $(\varphi,\sigma) \in H^{-\frac{1}{2}}(\partial\Omega) \times H^{-\frac{1}{2}}(\partial\Omega) \mapsto F((\varphi,\sigma))$ is a *quadratic functional*:

$$F((\varphi,\sigma)) := \frac{\mathrm{d}\widehat{\mathcal{E}}_F}{\mathrm{d}t}(\boldsymbol{\mathcal{V}};0)\,[\varphi,\sigma] = \mathsf{q}_{\boldsymbol{\mathcal{V}}}((\varphi,\sigma),(\varphi,\sigma)) + p_{\boldsymbol{\mathcal{V}}}(\varphi) + r_{\boldsymbol{\mathcal{V}}}(\sigma) \ , \tag{4.19}$$

with a bilinear form $\mathsf{q}_{\boldsymbol{\mathcal{V}}}$ on $H^{-\frac{1}{2}}(\partial\Omega) \times H^{-\frac{1}{2}}(\partial\Omega)$ and linear forms $p_{\boldsymbol{\mathcal{V}}}$ and $r_{\boldsymbol{\mathcal{V}}}$, given as

$$\mathsf{q}_{\boldsymbol{\mathcal{V}}}((\varphi,\sigma),(\varphi,\sigma)) \leftrightarrow \mathbf{T_2}(\varphi,\sigma) \quad , \quad p_{\boldsymbol{\mathcal{V}}}(\varphi) \leftrightarrow \mathbf{T_1}(\varphi) \quad , \tag{4.20}$$

$$r_{\boldsymbol{\mathcal{V}}}(\sigma) \leftrightarrow \mathbf{T_3}(\sigma) + \mathbf{T_4}(\sigma) + \mathbf{T_5}(\sigma) + \mathbf{T_6}(\sigma) \ , \tag{4.21}$$

in terms of the abbreviations from (4.17). Thus, F will be C^∞-smooth with first derivative

$$\mathsf{D}F((\varphi,\sigma))((\varphi',\sigma')) = \mathsf{q}_{\boldsymbol{\mathcal{V}}}((\varphi,\sigma),(\varphi',\sigma')) + \mathsf{q}_{\boldsymbol{\mathcal{V}}}((\varphi',\sigma'),(\varphi,\sigma)) + p_{\boldsymbol{\mathcal{V}}}(\varphi') + r_{\boldsymbol{\mathcal{V}}}(\sigma') \ , \tag{4.22}$$

and constant second derivative, if and only if $\mathsf{q}_{\boldsymbol{\mathcal{V}}}$ and $p_{\boldsymbol{\mathcal{V}}}$, $r_{\boldsymbol{\mathcal{V}}}$ are bounded on $H^{-\frac{1}{2}}(\partial\Omega) \times H^{-\frac{1}{2}}(\partial\Omega)$ and $H^{-\frac{1}{2}}(\partial\Omega)$, respectively.

From (4.22) we also learn that the adjoint variational problem (1.11) becomes: seek $(\nu,\kappa) \in H^{-\frac{1}{2}}(\partial\Omega) \times H^{-\frac{1}{2}}(\partial\Omega)$ such that

$$\mathsf{a}_V(\varphi,\nu) + \mathsf{a}_V(\sigma,\kappa) = \mathsf{q}_{\boldsymbol{\mathcal{V}}}((\psi,\rho),(\varphi,\sigma)) + \mathsf{q}_{\boldsymbol{\mathcal{V}}}((\varphi,\sigma),(\psi,\rho)) + p_{\boldsymbol{\mathcal{V}}}(\varphi) + r_{\boldsymbol{\mathcal{V}}}(\sigma) \tag{4.23}$$

for all $(\varphi,\sigma) \in H^{-\frac{1}{2}}(\partial\Omega) \times H^{-\frac{1}{2}}(\partial\Omega)$. A decoupling is possible: From the special structure of $\mathbf{T_2}$ we infer

$$\mathsf{q}_{\boldsymbol{\mathcal{V}}}((0,\sigma),(\varphi',\sigma')) = \mathsf{q}_{\boldsymbol{\mathcal{V}}}((\varphi,\sigma),(\varphi',0)) = 0 \quad \forall \varphi,\varphi',\sigma,\sigma' \in H^{-\frac{1}{2}}(\partial\Omega) \ .$$

This reveals that (4.23) is equivalent to the two decoupled variational equations

$$\mathsf{a}_V(\varphi,\nu) = \mathsf{q}_{\boldsymbol{\mathcal{V}}}((\varphi,0),(\psi,\rho)) + p_{\boldsymbol{\mathcal{V}}}(\varphi) \quad \forall \varphi \in H^{-\frac{1}{2}}(\partial\Omega) \ , \tag{4.24a}$$

$$\mathsf{a}_V(\sigma,\kappa) = \mathsf{q}_{\boldsymbol{\mathcal{V}}}((\psi,\rho),(0,\sigma)) + r_{\boldsymbol{\mathcal{V}}}(\sigma) \quad \forall \sigma \in H^{-\frac{1}{2}}(\partial\Omega) \ . \tag{4.24b}$$

Proposition 1.2 sends the message that for predicting superconvergence of forces it will be important to establish enhanced smoothness of the solutions ν and κ of (4.24). Therefore we have to understand the regularity of the right-hand sides of these variational equations.

4.4. **Mapping properties of Shape Derivative**

In this section we study the continuity of the quadratic functional $(\varphi,\sigma) \in H^{-\frac{1}{2}}(\partial\Omega) \times H^{-\frac{1}{2}}(\partial\Omega) \mapsto F((\varphi,\sigma)) := \frac{\mathrm{d}\widehat{\mathcal{E}}_F}{\mathrm{d}t}(\boldsymbol{\mathcal{V}};0)\,[\varphi,\sigma]$ from (4.19), (4.20). This boils down to establishing the continuity of its bilinear and linear terms $\mathsf{q}_{\boldsymbol{\mathcal{V}}}$, $p_{\boldsymbol{\mathcal{V}}}$, $r_{\boldsymbol{\mathcal{V}}}$ on the trace space $H^{-\frac{1}{2}}(\partial\Omega)$. We do this by a close inspection of the integral kernels occurring in (4.17). To avoid technical complications we impose smoothness requirements on $\boldsymbol{\mathcal{V}}$ and $\widetilde{g}$, which can certainly be relaxed.

Assumption 1. We assume that both $\boldsymbol{\mathcal{V}} \in \left(C_0^\infty(B)\right)^d$ and $\widetilde{g} \in C_0^\infty(B)$.

4.4.1. *Analysis of* $\mathsf{q}_{\boldsymbol{\mathcal{V}}}$

Using elementary properties of the fundamental solutions

$$G(\boldsymbol{x},\boldsymbol{y}) = \begin{cases} -\frac{1}{2\pi}\log\|\boldsymbol{x}-\boldsymbol{y}\| & \text{for } d=2\,, \\ \frac{1}{4\pi\|\boldsymbol{x}-\boldsymbol{y}\|} & \text{for } d=3\,, \end{cases} \quad \boldsymbol{\nabla}_{\boldsymbol{y}} G(\boldsymbol{x},\boldsymbol{y}) = \frac{1}{2^{d-1}\pi}\frac{\boldsymbol{x}-\boldsymbol{y}}{\|\boldsymbol{x}-\boldsymbol{y}\|^d}\,, \tag{4.25}$$

and the fact $\boldsymbol{\nabla}_{\boldsymbol{x}} G(\boldsymbol{x},\boldsymbol{y}) = -\boldsymbol{\nabla}_{\boldsymbol{y}} G(\boldsymbol{x},\boldsymbol{y})$ the term $\mathbf{T_2}$ from (4.17) can be recast as

$$\begin{aligned} \mathsf{q}_{\boldsymbol{\mathcal{V}}}((\varphi,\sigma),(\varphi',\sigma')) &= \int_{\partial\Omega}\int_{\partial\Omega} \varphi(\boldsymbol{y})\,\{\boldsymbol{\nabla}_{\boldsymbol{x}} G(\boldsymbol{x},\boldsymbol{y})\cdot\boldsymbol{\mathcal{V}}(\boldsymbol{x}) + \boldsymbol{\nabla}_{\boldsymbol{y}} G(\boldsymbol{x},\boldsymbol{y})\cdot\boldsymbol{\mathcal{V}}(\boldsymbol{y})\}\,\sigma'(\boldsymbol{x})\,\mathrm{d}S(\boldsymbol{y})\mathrm{d}S(\boldsymbol{x}) \\ &= -\frac{1}{2^{d-1}\pi}\int_{\partial\Omega}\int_{\partial\Omega} \varphi(\boldsymbol{y})\,\sigma'(\boldsymbol{x})\,\frac{\boldsymbol{x}-\boldsymbol{y}}{\|\boldsymbol{x}-\boldsymbol{y}\|^d}\cdot(\boldsymbol{\mathcal{V}}(\boldsymbol{x})-\boldsymbol{\mathcal{V}}(\boldsymbol{y}))\,\mathrm{d}S(\boldsymbol{x})\mathrm{d}S(\boldsymbol{y})\,. \end{aligned}$$

Thus, $\mathsf{q}_{\boldsymbol{\mathcal{V}}}$ can be expressed as

$$\mathsf{q}_{\boldsymbol{\mathcal{V}}}((\varphi,\sigma),(\varphi',\sigma')) = -\int_{\partial\Omega} \mathsf{V}(\varphi)(\boldsymbol{x})\,\sigma'(\boldsymbol{x})\,\mathrm{d}S(\boldsymbol{x})\,, \tag{4.26}$$

with an integral operator

$$\mathsf{V}(\psi)(\boldsymbol{x}) := \int_{\partial\Omega} K_V(\boldsymbol{x},\boldsymbol{x}-\boldsymbol{y})\,\psi(\boldsymbol{y})\mathrm{d}S(\boldsymbol{y})\,, \quad \boldsymbol{x}\in\partial\Omega\,, \tag{4.27a}$$

whose kernel is given by ($\boldsymbol{z} := \boldsymbol{x}-\boldsymbol{y}$)

$$K_V(\boldsymbol{x},\boldsymbol{z}) := \frac{1}{2^{d-1}\pi}\frac{\boldsymbol{z}}{\|\boldsymbol{z}\|^d}\cdot(\boldsymbol{\mathcal{V}}(\boldsymbol{x})-\boldsymbol{\mathcal{V}}(\boldsymbol{x}-\boldsymbol{z}))\,, \quad \boldsymbol{x},\boldsymbol{z}\in\mathbb{R}^d,\ \boldsymbol{z}\neq\mathbf{0}\,. \tag{4.27b}$$

Thanks to Assumption 1 we can insert a local Taylor expansion of $\boldsymbol{\mathcal{V}}$

$$\boldsymbol{\mathcal{V}}(\boldsymbol{x})-\boldsymbol{\mathcal{V}}(\boldsymbol{x}-\boldsymbol{z}) = \mathsf{D}\boldsymbol{\mathcal{V}}(\boldsymbol{x})\boldsymbol{z} - \frac{1}{2}\mathsf{D}^2\boldsymbol{\mathcal{V}}(\boldsymbol{x})(\boldsymbol{z},\boldsymbol{z}) + O(\|\boldsymbol{z}\|^3) \quad \text{for} \quad \boldsymbol{z}\to\mathbf{0}\,, \tag{4.28}$$

and the apparently strong singularity of the kernel can be canceled. For $d=2$ we find

$$K_V(\boldsymbol{x},\boldsymbol{z}) = K_0(\boldsymbol{x},\boldsymbol{z}) + \widetilde{K}_V(\boldsymbol{x},\boldsymbol{z})\,, \quad K_0(\boldsymbol{x},\boldsymbol{z}) := \frac{\boldsymbol{z}^\top\mathsf{D}\boldsymbol{\mathcal{V}}(\boldsymbol{x})\boldsymbol{z}}{2\pi\,||\boldsymbol{z}||^2}\,, \quad \boldsymbol{x},\boldsymbol{z}\in\mathbb{R}^2,\ \boldsymbol{z}\neq\mathbf{0}\,, \tag{4.29}$$

where

- $K_0(\boldsymbol{x},\boldsymbol{z})$ is smooth on $B\times\mathbb{R}^2\setminus\{\mathbf{0}\}$,
- $\boldsymbol{z}\in\mathbb{R}^2\setminus\{\mathbf{0}\}\mapsto\boldsymbol{\nabla}_{\boldsymbol{z}}K_0(\boldsymbol{x},\boldsymbol{z})$ is *homogeneous of degree* $-1=1-d$ and *odd*,
- $\boldsymbol{z}\mapsto\widetilde{K}_V(\boldsymbol{x},\boldsymbol{z})$ belongs to $W^{1,\infty}(\mathbb{R}^2)$ for all $\boldsymbol{x}\in B$.

According to [26, §4.3.3] this qualifies K_V as a *pseudo-homogeneous* kernel of class -1.

For $d=3$ we get (redefining notations)

$$K_V(\boldsymbol{x},\boldsymbol{z}) = \underbrace{\frac{\boldsymbol{z}^\top\mathsf{D}\boldsymbol{\mathcal{V}}(\boldsymbol{x})\boldsymbol{z}}{||\boldsymbol{z}||^3}}_{=:K_0(\boldsymbol{x},\boldsymbol{z})} - \frac{1}{2}\underbrace{\frac{\boldsymbol{z}^\top\mathsf{D}^2\boldsymbol{\mathcal{V}}(\boldsymbol{x})(\boldsymbol{z},\boldsymbol{z})}{||\boldsymbol{z}||^3}}_{=:K_1(\boldsymbol{x},\boldsymbol{z})} + \widetilde{K}_V(\boldsymbol{x},\boldsymbol{z})\,. \tag{4.30}$$

The terms satisfy that

- both K_0 and K_1 belong to $C^\infty(B\times\mathbb{R}^2\setminus\{\mathbf{0}\})$,
- $\boldsymbol{z}\in\mathbb{R}^2\setminus\{\mathbf{0}\}\mapsto\boldsymbol{\nabla}_{\boldsymbol{z}}K_0(\boldsymbol{z},\boldsymbol{z})$ is homogeneous of degree $-2=1-d$ and odd, and so is $\boldsymbol{z}\in\mathbb{R}^2\setminus\{\mathbf{0}\}\mapsto\mathsf{D}^2_{\boldsymbol{z}}K_1(\boldsymbol{x},\boldsymbol{z})$, and,

- again, $\boldsymbol{z} \mapsto \widetilde{K}_V(\boldsymbol{x},\boldsymbol{z})$ belongs to $W^{1,\infty}(\mathbb{R}^3)$ for all $\boldsymbol{x} \in B$.

As a consequence, also for $d = 3$, the kernel K_V meets the requirements of [26, §4.3.3] for being *pseudo-homogeneous* of class -1.

Now we can invoke [26, Thm. 4.3.2] together with results from [12, §1.3] on scales of Sobolev spaces $H^s(\partial\Omega)$ supported on boundaries of class $C^{r,1}$, $r \in \mathbb{N}_0$ [12, Def. 1.2.1.1].

Lemma 4.1. *Under Assumption 1 and for $\partial\Omega$ of class $C^{r,1}$, $r \in \mathbb{N}_0$, the boundary integral operator V as defined in (4.27) provides a bounded operator $H^{s-\frac{1}{2}}(\partial\Omega) \to H^{s+\frac{1}{2}}(\partial\Omega)$ for all $r - \frac{1}{2} \le s \le r + \frac{1}{2}$.*

This means that for $\partial\Omega$ of class $C^{r,1}$ the bilinear form $\mathsf{q}_{\boldsymbol{\mathcal{V}}}$ is continuous as a mapping

$$\mathsf{q}_{\boldsymbol{\mathcal{V}}} : \left(H^{-\frac{1}{2}+s}(\partial\Omega) \times H^{-\frac{1}{2}+s}(\partial\Omega)\right) \times \left(H^{-\frac{1}{2}-s}(\partial\Omega) \times H^{-\frac{1}{2}-s}(\partial\Omega)\right) \to \mathbb{R}\,, \tag{4.31}$$

for any $s \in [r - \frac{1}{2}, r + \frac{1}{2}]$.

4.4.2. *Analysis of $r_{\boldsymbol{\mathcal{V}}}$*

Inspecting (4.17) we see that the linear form $r_{\boldsymbol{\mathcal{V}}}$ as introduced in (4.20) can be expressed in terms of integral operators:

$$\begin{aligned} r_{\boldsymbol{\mathcal{V}}}(\sigma) = &\int_{\partial\Omega} \mathsf{R}(\widetilde{g}|_{\partial\Omega})(\boldsymbol{x})\,\sigma(\boldsymbol{x})\,\mathrm{d}S(\boldsymbol{x}) + \int_{\partial\Omega} \mathsf{K}(\boldsymbol{\nabla}\cdot(\widetilde{g}\boldsymbol{\mathcal{V}})|_{\partial\Omega})(\boldsymbol{x})\,\sigma(\boldsymbol{x})\,\mathrm{d}S(\boldsymbol{x}) \\ &- \frac{1}{2}\int_{\partial\Omega} \sigma(\boldsymbol{x})(\boldsymbol{\nabla}\widetilde{g}\cdot\boldsymbol{\mathcal{V}}(\boldsymbol{x}))\,\mathrm{d}S(\boldsymbol{x}) \end{aligned} \tag{4.32}$$

with integral operators

$$\mathsf{R}(f)(\boldsymbol{x}) := \int_{\partial\Omega} K_R(\boldsymbol{y},\boldsymbol{x}-\boldsymbol{y}) f(\boldsymbol{y})\,\mathrm{d}S(\boldsymbol{y})\,, \tag{4.33}$$

$$\begin{aligned} K_R(\boldsymbol{y},\boldsymbol{z}) := &-\left.\frac{\mathrm{d}\,\boldsymbol{\nabla}_{\boldsymbol{y}} G(\mathsf{T}^t_{\boldsymbol{\mathcal{V}}}(\boldsymbol{y}+\boldsymbol{z}),\mathsf{T}^t_{\boldsymbol{\mathcal{V}}}(\boldsymbol{y}))}{\mathrm{d}t}\right|_{t=0}\cdot\boldsymbol{n}(\boldsymbol{y}) \\ &+ \boldsymbol{\nabla}_{\boldsymbol{y}} G(\boldsymbol{y}+\boldsymbol{z},\boldsymbol{y})\cdot((\mathsf{D}\boldsymbol{\mathcal{V}}(\boldsymbol{y}))^\top \boldsymbol{n}(\boldsymbol{y}))\,,\quad \boldsymbol{z}\neq\mathbf{0}\,, \end{aligned}$$

$$\mathsf{K}(f)(\boldsymbol{x}) := \int_{\partial\Omega} K_K(\boldsymbol{y},\boldsymbol{x}-\boldsymbol{y}) f(\boldsymbol{y})\,\mathrm{d}S(\boldsymbol{y})\,, \tag{4.34}$$

$$K_K(\boldsymbol{y},\boldsymbol{z}) := \boldsymbol{\nabla}_{\boldsymbol{y}} G(\boldsymbol{y}+\boldsymbol{z},\boldsymbol{y})\cdot\boldsymbol{n}(\boldsymbol{y})\,,\quad \boldsymbol{z}\neq\mathbf{0}\,.$$

To begin with, the boundary integral operator K is the standard double-layer boundary integral operator for $-\Delta$ and, as such, $\mathsf{K} : H^s(\partial\Omega) \to H^s(\partial\Omega)$ is continuous for $-r-1 \le s \le r+1$, if $\partial\Omega$ is of class $C^{r,1}$ [25, Thms. 7.1 & 7.2].

We continue with an inspection of the kernels of the integral operator R using (4.25):

$$\begin{aligned} &-\left.\frac{\mathrm{d}\,\boldsymbol{\nabla}_{\boldsymbol{y}} G(\mathsf{T}^t_{\boldsymbol{\mathcal{V}}}(\boldsymbol{y}+\boldsymbol{z}),\mathsf{T}^t_{\boldsymbol{\mathcal{V}}}(\boldsymbol{y}))}{\mathrm{d}t}\right|_{t=0}\cdot\boldsymbol{n}(\boldsymbol{y}) + \boldsymbol{\nabla}_{\boldsymbol{y}} G(\boldsymbol{y}+\boldsymbol{z},\boldsymbol{y})\cdot((\mathsf{D}\boldsymbol{\mathcal{V}}(\boldsymbol{y}))^\top\boldsymbol{n}(\boldsymbol{y})) \\ &\quad= \frac{1}{2^{d-1}\pi}\left\{-\frac{\boldsymbol{n}(\boldsymbol{y})\cdot(\boldsymbol{\mathcal{V}}(\boldsymbol{y}+\boldsymbol{z})-\boldsymbol{\mathcal{V}}(\boldsymbol{y}))}{\|\boldsymbol{z}\|^d} + \mathrm{d}\,\frac{\boldsymbol{z}\cdot\boldsymbol{n}(\boldsymbol{y})\left(\boldsymbol{z}\cdot(\boldsymbol{\mathcal{V}}(\boldsymbol{y}+\boldsymbol{z})-\boldsymbol{\mathcal{V}}(\boldsymbol{y}))\right)}{\|\boldsymbol{z}\|^{d+2}}\right. \\ &\qquad\left. + \frac{\boldsymbol{z}}{\|\boldsymbol{z}\|^d}\cdot\mathsf{D}\boldsymbol{\mathcal{V}}(\boldsymbol{y})^\top\boldsymbol{n}(\boldsymbol{y})\right\}. \end{aligned} \tag{4.35}$$

Inserting the Taylor expansion

$$\boldsymbol{\mathcal{V}}(\boldsymbol{y}+\boldsymbol{z}) - \boldsymbol{\mathcal{V}}(\boldsymbol{y}) = \mathsf{D}\boldsymbol{\mathcal{V}}(\boldsymbol{y})\boldsymbol{z} + \frac{1}{2}\mathsf{D}^2\boldsymbol{\mathcal{V}}(\boldsymbol{y})(\boldsymbol{z},\boldsymbol{z}) + O(\|\boldsymbol{z}\|^3) \quad \text{for} \quad \boldsymbol{z}\to\mathbf{0}\,, \tag{4.36}$$

we are rewarded with a serendipitous cancellation of the third term and get (redefining notation from Section 4.4.1)

$$\begin{aligned} K_R(\boldsymbol{y},\boldsymbol{z}) = \frac{d}{2^{d-1}\pi} \underbrace{\frac{\boldsymbol{z}\cdot\boldsymbol{n}(\boldsymbol{y})}{\|\boldsymbol{z}\|^d}\,\frac{\boldsymbol{z}^\top \mathsf{D}\boldsymbol{\mathcal{V}}(\boldsymbol{y})\boldsymbol{z}}{\|\boldsymbol{z}\|^2}}_{=:K_0(\boldsymbol{y},\boldsymbol{z})} \\ + \frac{1}{2^{d-1}\pi} \underbrace{\left\{ -\frac{1}{2}\frac{\boldsymbol{n}(\boldsymbol{y})\cdot\mathsf{D}^2\boldsymbol{\mathcal{V}}(\boldsymbol{y})(\boldsymbol{z},\boldsymbol{z})}{\|\boldsymbol{z}\|^d} + \frac{d}{2}\frac{\boldsymbol{z}\cdot\boldsymbol{n}(\boldsymbol{y})}{\|\boldsymbol{z}\|^d}\,\frac{\boldsymbol{z}\cdot\mathsf{D}^2\boldsymbol{\mathcal{V}}(\boldsymbol{y})(\boldsymbol{z},\boldsymbol{z})}{\|\boldsymbol{z}\|^2} \right\}}_{=:K_1(\boldsymbol{y},\boldsymbol{z})} + \widetilde{K}_R(\boldsymbol{y},\boldsymbol{z})\,, \end{aligned} \tag{4.37}$$

for which we find that

- as functions of $(\boldsymbol{y},\boldsymbol{z})$ both K_0 and K_1 feature the same smoothness as the kernel K_K of the double-layer boundary integral operator,
- $\boldsymbol{z}\in\mathbb{R}^2\setminus\{\mathbf{0}\}\mapsto K_0(\boldsymbol{y},\boldsymbol{z})$ is odd and homogeneous of degree $1-d$,
- $\boldsymbol{z}\in\mathbb{R}^2\setminus\{\mathbf{0}\}\mapsto \boldsymbol{\nabla}_{\boldsymbol{z}}K_1(\boldsymbol{y},\boldsymbol{z})$ is odd and homogeneous of degree $1-d$,
- and $\widetilde{K}_R\in W^{1,\infty}(\partial\Omega\times\mathbb{R}^2)$.

We conclude that K_R is a *pseudo-homogeneous* integral kernel of class 0 in the sense of [26, §4.3.3], which means that the integral operator R enjoys the same continuity properties as K: It maps continuously $H^s(\partial\Omega)\to H^s(\partial\Omega)$ for $-r-1\le s\le r+1$, if $\partial\Omega$ is of class $C^{r,1}$ [26, Thm. 4.3.2].

Summing up, under Assumption 1 for $\partial\Omega$ of class $C^{r,1}$ this ensures

$$\mathsf{R}(\widetilde{g}|_{\partial\Omega})\in H^{r+1}(\partial\Omega) \quad , \quad \mathsf{K}(\boldsymbol{\nabla}\cdot(\widetilde{g}\boldsymbol{\mathcal{V}})|_{\partial\Omega})\in H^{r+1}(\partial\Omega)\,,$$

which means that $r_{\boldsymbol{\mathcal{V}}}$ is a continuous linear functional on $H^{-r-1}(\partial\Omega)$, which, by duality, can be identified with a function in $H^{r+1}(\partial\Omega)$.

4.4.3. *Analysis of $p_{\boldsymbol{\mathcal{V}}}$*

The simple formula

$$p_{\boldsymbol{\mathcal{V}}}(\varphi) = \frac{1}{2}\int_{\partial\Omega}\varphi(\boldsymbol{x})(\boldsymbol{\nabla}\widetilde{g}(\boldsymbol{x})\cdot\boldsymbol{\mathcal{V}}(\boldsymbol{x}))\,\mathrm{d}S(\boldsymbol{x}) \tag{4.38}$$

combined with the smoothness assumption Assumption 1 for $\widetilde{g}$ and $\boldsymbol{\mathcal{V}}$ means that $p_{\boldsymbol{\mathcal{V}}}$ is a continuous linear functional on $H^{-s}(\partial\Omega)$ for $s=r+1$, if $\partial\Omega$ is of class $C^{r,1}$. Thus, by duality, $p_{\boldsymbol{\mathcal{V}}}$ can be regarded as an element of $H^{r+1}(\partial\Omega)$.

4.5. **Section 4.3 continued: BEM-Based Approximation of Forces**

As announced in Section 2.2, we consider only the lowest-order boundary element space $\mathcal{S}_0^{-1}(\partial\Omega_h)$ of $\partial\Omega_h$-piecewise constant functions. Then, Proposition 1.2 gives us the following concrete estimate

for the error of the computed force in the direction $\boldsymbol{\mathcal{V}}$: With a constant $C > 0$ independent of the boundary element space

$$\left| \frac{\mathrm{d}\widehat{\mathcal{E}}_F}{\mathrm{d}t}(\boldsymbol{\mathcal{V}};0)\,[\psi,\rho] - \frac{\mathrm{d}\widehat{\mathcal{E}}_F}{\mathrm{d}t}(\boldsymbol{\mathcal{V}};0)\,[\psi_h,\rho_h] \right| \leq CE_1(E_2+E_1)\;, \tag{4.39}$$

with the best approximation error norms, which are equal to the Galerkin discretization error by Cea's lemma [30, §8.1, Thm. 8.1]

$$\begin{aligned} E_1 &:= \inf_{\psi_h \in \mathcal{S}_0^{-1}(\partial\Omega_h)} \|\psi-\psi_h\|_{H^{-\frac{1}{2}}(\partial\Omega)} + \inf_{\rho_h \in \mathcal{S}_0^{-1}(\partial\Omega_h)} \|\rho-\rho_h\|_{H^{-\frac{1}{2}}(\partial\Omega)}\;, \\ E_2 &:= \inf_{\kappa_h \in \mathcal{S}_0^{-1}(\partial\Omega_h)} \|\kappa-\kappa_h\|_{H^{-\frac{1}{2}}(\partial\Omega)} + \inf_{\nu_h \in \mathcal{S}_0^{-1}(\partial\Omega_h)} \|\nu-\nu_h\|_{H^{-\frac{1}{2}}(\partial\Omega)}\;, \end{aligned}$$

where $\psi,\rho,\nu,\kappa \in H^{-\frac{1}{2}}(\partial\Omega)$ are the solutions of (2.1), (4.11), (4.24a), and (4.24b), respectively.

For the following discussion we maintain Assumption 1 and also assume that $\partial\Omega$ is of class $C^{r,1}$, $r \in \mathbb{N}_0$, which entails that

- the right-hand side of the BIE (2.1) can be regarded as a function in $H^{r+1}(\partial\Omega)$,
- the right-hand side of the adjoint variational problem (4.11) belongs to $H^{r+1}(\partial\Omega)$, too,
- by the results from Section 4.4.3 the right-hand side of (4.24a) is in $H^{r+1}(\partial\Omega)$, and,
- as we have seen in Section 4.4.1 and Section 4.4.2, the right-hand side of (4.24b) corresponds to a an element of $H^{\min\{s+1,r+1\}}(\partial\Omega)$, if $\psi \in H^s(\partial\Omega)$.

By the following elliptic lifting theorem for the single-layer boundary integral equation, regularity of the right-hand sides can be transferred to solutions.

Theorem 4.2 ([25, Thm. 7.16]). *Given $f \in H^{\frac{1}{2}}(\partial\Omega)$ let $\eta \in H^{-\frac{1}{2}}(\partial\Omega)$ be the solution of*

$$\mathsf{a}_V(\eta,\varphi) = \int_{\partial\Omega} f(\boldsymbol{x})\varphi(\boldsymbol{x})\,\mathrm{d}S(\boldsymbol{x}) \quad \forall \varphi \in H^{-\frac{1}{2}}(\partial\Omega)\;,$$

the integral to be read as duality pairing. Then extra smoothness of f induces more regularity of η:

(i) If $\partial\Omega$ is Lipschitz, $f \in H^1(\partial\Omega)$, then $\eta \in L^2(\partial\Omega)$.

(ii) If $\partial\Omega$ is of class $C^{r,1}$, $r \in \mathbb{N}$, and $f \in H^{r+\frac{1}{2}}(\partial\Omega)$, then $\eta \in H^{r-\frac{1}{2}}(\partial\Omega)$.

In addition, in [28, §4.3.4] we find the following approximation estimate for piecewise smooth $\partial\Omega$ and shape-regular sequences of meshes

$$\inf_{\varphi_h \in \mathcal{S}_0^{-1}(\partial\Omega_h)} \|\varphi-\varphi_h\|_{H^{-\frac{1}{2}}(\partial\Omega)} \leq Ch^{\min\{1,s\}+\frac{1}{2}} \|\varphi\|_{H^s(\partial\Omega)} \quad \forall \varphi \in H^s(\partial\Omega)\;, \tag{4.40}$$

where h stands for the mesh width of $\partial\Omega_h$. We discuss two cases.

(I) If $\partial\Omega$ is of class $C^{r,1}$ with $r \in \mathbb{N}$, then Theorem 4.2 together with the right-hand side regularities listed above yields

$$\psi,\rho,\nu,\kappa \in H^{r-\frac{1}{2}}(\partial\Omega)\;.$$

The $\mathcal{S}_0^{-1}(\partial\Omega_h)$ best-approximation errors in the $H^{-\frac{1}{2}}(\partial\Omega)$-norm for all of these functions will converge like $O(h^{\min\{\frac{3}{2},r\}})$ for $h \to 0$, for instance on sequences of uniformly refined meshes. Plugging this into (4.39), we end up with

$$\left| \frac{\mathrm{d}\widehat{\mathcal{E}}_F}{\mathrm{d}t}(\boldsymbol{\mathcal{V}};0)\,[\psi,\rho] - \frac{\mathrm{d}\widehat{\mathcal{E}}_F}{\mathrm{d}t}(\boldsymbol{\mathcal{V}};0)\,[\psi_h,\rho_h] \right| = O(h^{\min\{3,2r\}}) \quad \text{for} \quad h \to 0\;. \tag{4.41}$$

(II) If we merely know that $\partial\Omega$ is Lipschitz, we can still conclude

$$\psi, \rho, \nu, \kappa \in L^2(\partial\Omega) ,$$

and the $H^{-\frac{1}{2}}(\partial\Omega)$-norms of the best approximation errors decay asymptotically like $O(h^{\frac{1}{2}})$ for $h \to 0$. By (4.39) this involves a minimal $O(h)$ -convergence of the error in the force.

Remark 4.3. The above crude convergence estimates can be refined for piecewise smooth domains taking into account the special corner and edge singular functions present in the solutions of the variational problems [7]. This a-priori knowledge about the structure of the solution can be exploited through the use of algebraically graded meshes, see [13, Ch. 7], [10], [27], in a BEM framework with fixed polynomial degree, or by employing geometrically graded meshes combined with *hp*-BEM, see [31, 18, 23] and [13, Ch. 8]. A flexible alternative is adaptive mesh refinement controlled by an a-posteriori error estimator, refer to [2] and the references therein.

Remark 4.4. Throughout this section we took for granted a given fixed smooth displacement field $\boldsymbol{\mathcal{V}}$. As an extension of the investigations in this section one could also aim for $\boldsymbol{\mathcal{V}}$-uniform estimates of the approximation error for shape derivatives as has been done in [21].

5. Numerical Experiments

Now we study the convergence of the new pullback approach formula from (4.17) empirically. The convergence studies are done in 2D entirely and are divided into two parts. In the first part we restrict ourselves to physically meaningful quantities: net forces and torques. In the second part, aligned with our view of force as a shape derivative, a linear functional on displacements, we examine the convergence of a dual norm of the approximation error.

5.1. Implementation

Both the pullback approach formula (4.17) and the stress tensor formula (3.9) were implemented using exact parametrizations for the boundaries[6]. Quasi-uniform sequences of mesh partitions of $\partial\Omega$ were employed with increasing resolution. As explained in Section 2.2 and Section 4.3, boundary-element Galerkin discretization with trial and test space $\mathcal{S}_0^{-1}(\partial\Omega_h)$ is employed to solve the variational equations (2.1) and (4.11) approximately. The obtained solutions ψ_h and ρ_h are used to compute approximations of the forces according to (4.18). For the evaluation of integrals with singular kernels we use log weighted gauss quadrature and regularization by transformation to polar coordinates [14, §9.4.5]. All integrals with smooth integrands are evaluated using Gauss quadrature of order 16. The required derivatives of $\widetilde{g}$ and $\boldsymbol{\mathcal{V}}$ are assumed to be explicitly available in the implementation.

5.2. Total Force and Torque

Experiment 3. We use the same geometric settings as introduced already in Experiment 1. In particular we use $\widetilde{g} \equiv 1$ close to ∂D and $\widetilde{g} \equiv 0$ close to ∂B. For constant Dirichlet data we compute the total force according to (3.7) based on the deformation fields discussed in REMARK 3.3. We employ both (4.17) ("Pullback approach (BEM)") and (3.9) ("Stress tensor (BEM)") on a quasi-uniform sequence of meshes of $\partial\Omega_h$. As before we monitor the Euclidean norm of the error in the total force as a function of the mesh width. As reference bona-fide close-to-exact solution we used the total force computed by the pullback approach on a uniform mesh with 9000 (kite-shaped D)/7200

[6]Code available at https://gitlab.ethz.ch/ppanchal/fcsc.git. Instructions on how to repeat some of the numerical experiments of this section are given in a README file.

(square-shaped D) cells. The resulting error curves are added to the plots of Experiment 2 and are shown in Figure 5.1 for comparison.

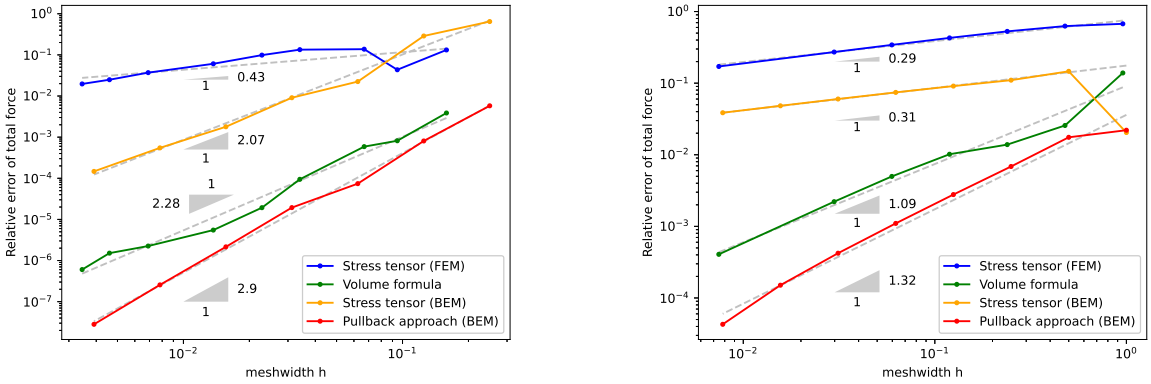

(A) Kite-shaped D (B) Square-shaped D

FIGURE 5.1. Error of $S_0^{-1}(\partial\Omega_h)$ - BEM based forces as a function of the meshwidth h of $\partial\Omega_h$. Dashed lines represent the linear regression fit.

We see that the pullback approach outperforms every other method not only in terms of the absolute accuracy but also in terms of the asymptotic rate of (algebraic) convergence. For the smooth kite-shaped D (Figure 5.1 (A)) it achieves the optimal convergence $O(h^3)$ for $h \to 0$ predicted in Section 4.5. For the square-shaped D (Figure 5.1 (A)) strong singularities of the electrostatic potential u at the re-entrant corners make the rates of convergence deteriorate substantially for all methods, with the pullback approach maintaining its clear lead.

Remark 5.1. The surprisingly good performance of the BEM-based evaluation of the stress tensor formula (3.9) for smooth Γ remains a mystery. It reminds us of a similarly unexpected fast convergence of a boundary-based shape-derivative formula reported in [21, §4] and, later, theoretically explained in [11, §3.2].

Experiment 4. In the setting of Experiment 3 we also compute the net torque on D according to (3.8), with $\boldsymbol{c} = (0.5, 0)^\top$ for square-shaped D and $\boldsymbol{c} = (0.38, 0.5)^\top$ for kite-shaped D, using the pullback approach (4.17) and stress tensor formula (BEM) (3.9). The errors of the approximate torques are plotted against the meshwidth h in Figure 5.2.

The observations closely match those made in Experiment 3. The pullback approach gives the best results both in terms of absolute accuracy and in terms of asymptotic rate of convergence. Its advantage is more pronounced for non-smooth D.

5.3. Approximation of Force Functionals

Experiment 5. Inspired by [21, §4] we consider the dual norm of the force as a linear mapping from displacements $\boldsymbol{\mathcal{V}}$ to the real numbers over a finite dimensional subspace W_N of $\left(H^1(B)\right)^2$ and measure the error

$$\text{err} := \max_{\boldsymbol{\mathcal{V}} \in W_N} \frac{1}{\|\boldsymbol{\mathcal{V}}\|_{H^1(B)}} \left| \frac{\mathrm{d}\widehat{\mathcal{E}}_F}{\mathrm{d}t}(\boldsymbol{\mathcal{V}}; 0)\,[\psi, \rho] - \frac{\mathrm{d}\widehat{\mathcal{E}}_F}{\mathrm{d}t}(\boldsymbol{\mathcal{V}}; 0)\,[\psi_h, \rho_h] \right|, \tag{5.1}$$

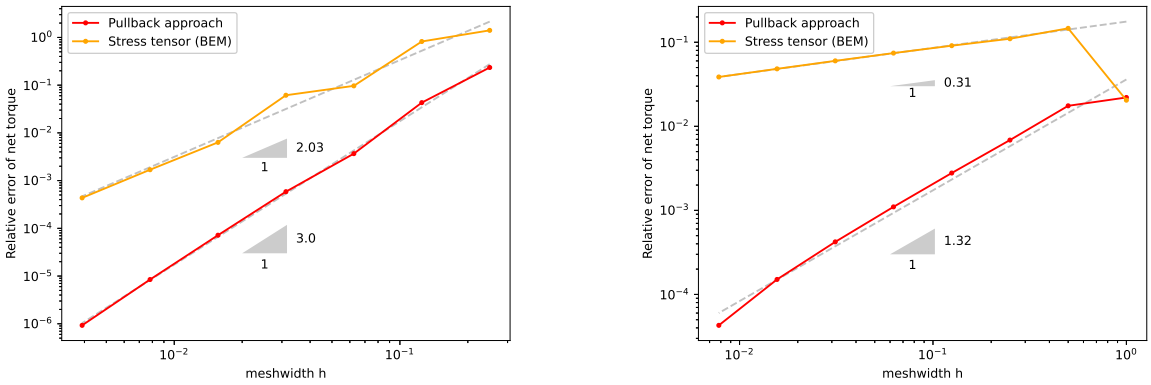

(A) Kite-shaped D (B) Square-shaped D

FIGURE 5.2. Errors of $S_0^{-1}(\partial\Omega_h)$ - BEM based torques by (4.17) ("Pullback approach") and (3.9) ("Stress tensor (BEM)") as a function of the meshwidth h of $\partial\Omega_h$

both for the pullback approach (4.17) and stress tensor (BEM) (3.9). We adopt the setting of Experiment 3 and we use the same BEM to compute $\psi_h, \rho_h \in \mathcal{S}_0^{-1}(\partial\Omega_h)$. Two choices for $W_N := U \times U$ are used in this numerical experiment,

$$\text{(I)} \qquad U := \operatorname{span}\{\boldsymbol{x} = (x,y)^\top \mapsto x^m y^n,\ 1 \le m,n \le 5\}\ , \tag{5.2}$$

$$\text{(II)} \qquad U := \operatorname{span}\{\boldsymbol{x} = (x,y)^\top \mapsto \sin(mx)\sin(ny),\ 1 \le m,n \le 5\}\ . \tag{5.3}$$

As reference solutions we use the directional forces obtained by the pullback approach on meshes created by one more step of refinement. The dual norms (5.1) are plotted in Figure 5.3.

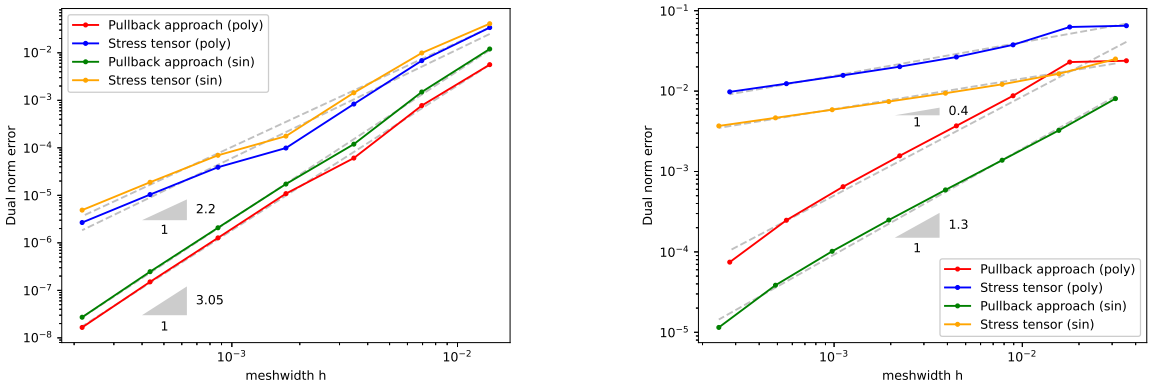

(A) Kite-shaped D (B) Square-shaped D

FIGURE 5.3. Dual norm errors (5.1) for polynomial (poly) and sinusoidal (sin) basis, as a function of the meshwidth h of $\partial\Omega_h$. Dashed lines represent the linear regression fit.

Obviously, the BEM-based pullback approach (4.17) offers better accuracy also in the approximate dual norm, but for the kite-shaped D the stress tensor formula (3.9) achieves similar empiric rates

of convergence for $h \to 0$. We cannot offer an explanation for this surprising observation. Conversely, for the square-shaped D the pullback approach is much better also in terms of the rate of asymptotic (algebraic) convergence. It seems to be less affected by the presence of strong corner singularities in ψ and ρ.

Experiment 6. In Section 4 we had always taken for granted that the Dirichlet data g possess a sufficiently regular extension $\widetilde{g}$ to the hold-all domain B. In this experiment we demonstrate the importance of the smoothness of $\tilde{g}$ as regards the approximations of shape derivatives. The experiment shown next uses two different functions $\tilde{g}_1$ and $\tilde{g}_2$ such that $\tilde{g}_1|_\Gamma = \tilde{g}_2|_\Gamma = g$. We work with the model geometry of the square-shaped D from Experiment 1 and with $g = 1$. For imposing $g = 1$ on Γ we use $\tilde{g}_1 \equiv 1$ in a neighborhood of Γ and for $\tilde{g}_2$ we use four corner singular functions located at the four corners of the square shaped D. These corner singular functions are rotations and reflections of the simple function

$$(r, \theta) \mapsto r^{\frac{2}{3}} \sin\left(\frac{2}{3}\theta\right) \quad \text{(polar coordinates)} ,$$

which is harmonic but its gradient blows up for $r \to 0$. By comparing the green and red curves in Figure 5.4 we see that a smoother g drastically improves the performance of the pullback approach (4.17) as regards both absolute accuracy and the asymptotic (algebraic) convergence rates. For the case of stress tensor formula (3.9), a smoother g makes little difference.

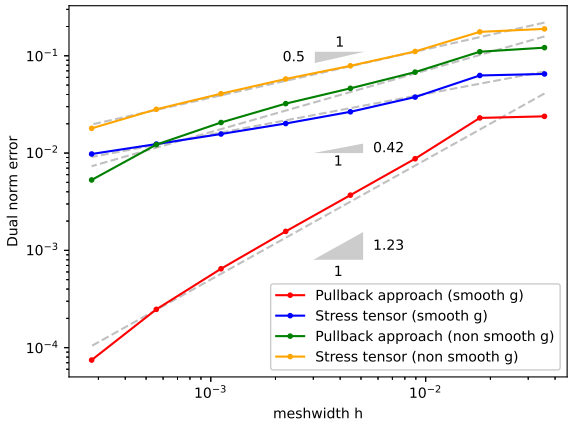

Figure 5.4. Dual norm errors (5.1) with polynomial basis, using a smooth and non-smooth $\widetilde{g}$, as a function of the meshwidth h of $\partial\Omega_h$

6. Conclusion

In this work we have demonstrated how fast and robust convergence of approximate forces in the context of boundary-element approximations of electrostatic potential boundary value problems can be achieved by new formulas that merely involve functions and integrals defined on the boundary. On the one hand, these formulas entail the solution of an adjoint discrete boundary integral equation and the evaluation of a few singular integrals. On the other hand, in particular in the case of only piecewise smooth boundaries, they are superior to the simple and classical force formulas obtained from the Maxwell stress tensor. In our opinion this gain in accuracy and robustness outweighs the extra cost.

Techniques from shape calculus paved the way to our new formulas. We expect that these techniques can also yield new and better formulas for magnetic forces and general electromagnetic forces in dynamic settings.

Appendix A. Derivation of Boundary-Based Shape Derivative Formula (3.9)

We start from a mixed variational formulation of (1.1) in $H^1(B) \times \boldsymbol{H}(\mathrm{div}0, B)$ [30, §4.1.2]. We seek $(u, \boldsymbol{\mu}) \in H^1(B) \times \boldsymbol{H}(\mathrm{div}0, B)$ such that

$$\int_\Omega \boldsymbol{\nabla} u \cdot \boldsymbol{\nabla} v \, \mathrm{d}\boldsymbol{x} + \int_{\partial\Omega} v \, \boldsymbol{\mu} \cdot \boldsymbol{n} \, \mathrm{d}S = 0 \qquad \forall v \in H^1(B) \, , \tag{A.1}$$

$$\int_{\partial\Omega} u \, \boldsymbol{\lambda} \cdot \boldsymbol{n} \, \mathrm{d}S = \int_\Gamma g \, \boldsymbol{\lambda} \cdot \boldsymbol{n} \, \mathrm{d}S \qquad \forall \boldsymbol{\lambda} \in \boldsymbol{H}(\mathrm{div}0, B) \, , \tag{A.2}$$

where $g = \widetilde{g}|_\Gamma$ for a $\widetilde{g} \in H^1(B)$ that vanishes on ∂B. There is a unique solution only for u but not for the Lagrange multiplier $\boldsymbol{\mu}$. We define the associated symmetric bilinear form a and linear form $l_{\widetilde{g}}$ for $(w, \boldsymbol{\kappa}), (v, \boldsymbol{\lambda}) \in H^1(B) \times \boldsymbol{H}(\mathrm{div}0, B)$:

$$\mathsf{a}((w, \boldsymbol{\kappa}), (v, \boldsymbol{\lambda})) := \int_\Omega \boldsymbol{\nabla} w \cdot \boldsymbol{\nabla} v \, \mathrm{d}\boldsymbol{x} + \int_{\partial\Omega} v \, \boldsymbol{\kappa} \cdot \boldsymbol{n} \, \mathrm{d}S + \int_{\partial\Omega} u \, \boldsymbol{\lambda} \cdot \boldsymbol{n} \, \mathrm{d}S \, , \tag{A.3}$$

$$l_{\widetilde{g}}((v, \boldsymbol{\lambda})) := \int_\Gamma g \, \boldsymbol{\lambda} \cdot \boldsymbol{n} \, \mathrm{d}S \, . \tag{A.4}$$

The system in (A.1) can be compactly written as: Seek $(u, \boldsymbol{\mu}) \in H^1(B) \times \boldsymbol{H}(\mathrm{div}0, B)$:

$$\mathsf{a}((u, \boldsymbol{\mu}), (v, \boldsymbol{\lambda})) = l_{\widetilde{g}}((v, \boldsymbol{\lambda})) \quad \forall (v, \boldsymbol{\lambda}) \in H^1(B) \times \boldsymbol{H}(\mathrm{div}0, B) \, . \tag{A.5}$$

We use the energy functional from (3.1) in the volume integral form:

$$\mathcal{E}_F(\Omega) := \frac{1}{2} \int_\Omega \|\boldsymbol{\nabla} u(\boldsymbol{x})\|^2 \, \mathrm{d}\boldsymbol{x} = \frac{1}{2} \mathsf{a}((u, \boldsymbol{0}), (u, \boldsymbol{0})) \, , \tag{A.6}$$

where $u = u(\Omega)$ solves (A.1). Following the definitions in Section 4.1, we write $\left(\Omega_t := \mathsf{T}^t_{\boldsymbol{\mathcal{V}}}(\Omega)\right)_{|t|<\delta}$ for the 1-parameter family of slightly deformed domains induced by a given deformation vector field $\boldsymbol{\mathcal{V}} \in \left(C_0^\infty(B)\right)^d$. Replacing $\Omega \to \Omega_t$, $\partial\Omega \to \partial\Omega_t$ and $\Gamma \to \Gamma_t$ in (A.3) yields a t-dependent version of its constituent parts. For $(w, \boldsymbol{\kappa}), (v, \boldsymbol{\lambda}) \in H^1(B) \times \boldsymbol{H}(\mathrm{div}0, B)$:

$$\mathsf{a}(t; (w, \boldsymbol{\kappa}), (v, \boldsymbol{\lambda})) := \int_{\Omega_t} \boldsymbol{\nabla} w \cdot \boldsymbol{\nabla} v \, \mathrm{d}\boldsymbol{x} + \int_{\partial\Omega_t} v \, \boldsymbol{\kappa} \cdot \boldsymbol{n} \, \mathrm{d}S + \int_{\partial\Omega_t} u \, \boldsymbol{\lambda} \cdot \boldsymbol{n} \, \mathrm{d}S \, , \tag{A.7}$$

$$l_{\widetilde{g}}(t; (v, \boldsymbol{\lambda})) := \int_{\Gamma_t} \widetilde{g} \, \boldsymbol{\lambda} \cdot \boldsymbol{n} \, \mathrm{d}S \, . \tag{A.8}$$

The t dependent energy functional is given as

$$\mathcal{E}_F(t) := J(t; (u(t), \boldsymbol{\mu}(t))) \, , \quad J(t; (w, \boldsymbol{\kappa})) := \frac{1}{2} \mathsf{a}(t; (w, \boldsymbol{0}), (w, \boldsymbol{0})) \, , \tag{A.9}$$

where $(u(t), \boldsymbol{\mu}(t)) \in H^1(B) \times \boldsymbol{H}(\mathrm{div}0, B)$ solves the state problem on Ω_t:

$$\mathsf{a}(t; (u(t), \boldsymbol{\mu}(t)), (v, \boldsymbol{\lambda})) = l_{\widetilde{g}}(t; (v, \boldsymbol{\lambda})) \quad \forall (v, \boldsymbol{\lambda}) \in H^1(B) \times \boldsymbol{H}(\mathrm{div}0, B) \, . \tag{A.10}$$

Notice that in this derivation, the function space framework is already independent of t. Following the adjoint approach [19, §1.6.4] from Section 4.2, we can define the relevant Lagrangian. For $(w, \boldsymbol{\kappa}), (v, \boldsymbol{\lambda}) \in H^1(B) \times \boldsymbol{H}(\mathrm{div}0, B)$:

$$L(t; (w, \boldsymbol{\kappa}), (v, \boldsymbol{\lambda})) := J(t; (w, \boldsymbol{\kappa})) + \mathsf{a}(t; (w, \boldsymbol{\kappa}), (v, \boldsymbol{\lambda})) - l_{\widetilde{g}}(t; (v, \boldsymbol{\lambda})) \, . \tag{A.11}$$

Plugging in $(w, \boldsymbol{\kappa}) = (u(t), \boldsymbol{\mu}(t))$, the solution for (A.10), we recover an expression for the field energy

$$\mathcal{E}_F(t) = L(t; (u(t), \boldsymbol{\mu}(t)), (v, \boldsymbol{\lambda})) \quad \forall (v, \boldsymbol{\lambda}) \in H^1(B) \times \boldsymbol{H}(\mathrm{div}0, B) \,. \tag{A.12}$$

Exploiting the freedom to choose $(v, \boldsymbol{\lambda})$, we choose it as the adjoint solution $(\rho, \boldsymbol{\pi}) \in H^1(B) \times \boldsymbol{H}(\mathrm{div}0, B)$ such that

$$\mathsf{a}(0; (v, \boldsymbol{\lambda}), (\rho, \boldsymbol{\pi})) = -\left\langle \frac{\partial J}{\partial (w, \boldsymbol{\kappa})}(0; (u(0), \boldsymbol{\mu}(0))), (v, \boldsymbol{\lambda}) \right\rangle \quad \forall (v, \boldsymbol{\lambda}) \in H^1(B) \times \boldsymbol{H}(\mathrm{div}0, B) \tag{A.13}$$

$$\iff \qquad \mathsf{a}((v, \boldsymbol{\lambda}), (\rho, \boldsymbol{\pi})) = -\mathsf{a}((v, \mathbf{0}), (u, \mathbf{0})) \quad \forall (v, \boldsymbol{\lambda}) \in H^1(B) \times \boldsymbol{H}(\mathrm{div}0, B) \,, \tag{A.14}$$

where we used $u(0) = u$ and $\boldsymbol{\mu}(0) = \boldsymbol{\mu}$. The equations can easily be decoupled by putting $v = 0$ or $\boldsymbol{\lambda} = \mathbf{0}$. Thus we see that adjoint solution is $(\rho, \boldsymbol{\pi}) = (0, -\boldsymbol{\nabla} u)$. Now the shape derivative can be computed using only the partial derivatives with respect to t:

$$\frac{\mathrm{d}\mathcal{E}_F}{\mathrm{d}t}(0) = \frac{\partial L}{\partial t}(0; (u, \boldsymbol{\mu}), (0, -\boldsymbol{\nabla} u)) = \frac{\partial J}{\partial t}(0; (u, \boldsymbol{\mu})) + \frac{\partial \mathsf{a}}{\partial t}(0; (u, \boldsymbol{\mu}), (0, -\boldsymbol{\nabla} u)) - \frac{\partial l_{\widetilde{g}}}{\partial t}(0; (0, -\boldsymbol{\nabla} u)) \,. \tag{A.15}$$

Using the identities in Section 4.2 and [9, Ch. 9, Thm. 4.1], the *partial derivatives* with respect to t can be easily computed, because the integrands are independent of t:

$$\frac{\partial J}{\partial t}(0; (u, \boldsymbol{\mu})) = \frac{1}{2} \int_\Gamma \|\boldsymbol{\nabla} u\|^2 (\boldsymbol{\mathcal{V}} \cdot \boldsymbol{n}) \, \mathrm{d}S \,, \tag{A.16}$$

$$\frac{\partial \mathsf{a}}{\partial t}(0; (u, \boldsymbol{\mu}), (0, -\boldsymbol{\nabla} u)) = -\int_\Gamma \|\boldsymbol{\nabla} u\|^2 (\boldsymbol{\mathcal{V}} \cdot \boldsymbol{n}) \, \mathrm{d}S \,, \tag{A.17}$$

$$\frac{\partial l_{\widetilde{g}}}{\partial t}(0; (0, -\boldsymbol{\nabla} u)) = -\int_\Gamma \boldsymbol{\nabla} u \cdot \boldsymbol{\nabla} \widetilde{g} \, (\boldsymbol{\mathcal{V}} \cdot \boldsymbol{n}) \, \mathrm{d}S \,. \tag{A.18}$$

Summing up and using the fact that $\boldsymbol{\nabla} \widetilde{g} - \boldsymbol{\nabla} u$ is in the normal direction at the surface, we get the shape derivative:

$$\frac{\mathrm{d}\mathcal{E}_F}{\mathrm{d}\Omega}(\Omega; \boldsymbol{\mathcal{V}}) = \frac{1}{2} \int_\Gamma \left(((\boldsymbol{\nabla} \widetilde{g} - \boldsymbol{\nabla} u) \cdot \boldsymbol{n})(\boldsymbol{\nabla} u \cdot \boldsymbol{n}) + \boldsymbol{\nabla} \widetilde{g} \cdot \boldsymbol{\nabla} u \right) (\boldsymbol{\mathcal{V}} \cdot \boldsymbol{n}) \, \mathrm{d}S \,. \tag{A.19}$$

Appendix B. Derivation of Volume-based Shape Derivative Formula

We start from the variational formulation of (1.1) in the Sobolev space $H^1_0(\Omega)$ using $w := u - \widetilde{g} \in H^1_0(\Omega)$:

$$w \in H^1_0(\Omega): \quad \mathsf{a}(w, v) := \int_\Omega \boldsymbol{\nabla} w \cdot \boldsymbol{\nabla} v \, \mathrm{d}\boldsymbol{x} = l_{\widetilde{g}}(v) := -\int_\Omega \boldsymbol{G} \cdot \boldsymbol{\nabla} v \, \mathrm{d}\boldsymbol{x} \quad \forall v \in H^1_0(\Omega) \,, \tag{B.1}$$

where $g = \widetilde{g}|_\Gamma$ for a $\widetilde{g} \in H^1(\Omega)$ that vanishes on ∂B and $\boldsymbol{G} := \boldsymbol{\nabla} \widetilde{g}$. By the Lax-Milgram lemma [5, §6.2] existence and uniqueness of w is guaranteed. We use the energy functional from (3.1) in the volume integral form

$$\mathcal{E}_F(\Omega) := \frac{1}{2} \int_\Omega \|\boldsymbol{\nabla} u(\boldsymbol{x})\|^2 \, \mathrm{d}\boldsymbol{x} = \frac{1}{2} \int_\Omega \|\boldsymbol{\nabla} w(\boldsymbol{x}) + \boldsymbol{G}(\boldsymbol{x})\|^2 \, \mathrm{d}\boldsymbol{x} \,, \tag{B.2}$$

where $w = w(\Omega)$ solves (B.1). Following the definitions in Section 4.1, we write $\left(\Omega_t := \mathsf{T}^t_{\boldsymbol{\mathcal{V}}}(\Omega)\right)_{|t|<\delta}$ for the 1-parameter family of slightly deformed domains induced by a given deformation vector field $\boldsymbol{\mathcal{V}} \in \left(C^\infty_0(B)\right)^d$. Considering $\widetilde{g} \in H^1_0(B)$ and replacing $\Omega \to \Omega_t$ in (B.1) yields a t-dependent version:

$$w(t) \in H^1_0(\Omega_t): \quad \mathsf{a}(t; w(t), v) = l_{\widetilde{g}}(t; v) \quad \forall v \in H^1_0(\Omega_t) \,, \tag{B.3}$$

where, for $w, v \in H^1_0(\Omega_t)$,

$$\mathsf{a}(t; w, v) := \int_{\Omega_t} \boldsymbol{\nabla} w \cdot \boldsymbol{\nabla} v \, \mathrm{d}\boldsymbol{x}, \quad l_{\widetilde{g}}(t; v) := -\int_{\Omega_t} \boldsymbol{G} \cdot \boldsymbol{\nabla} v \, \mathrm{d}\boldsymbol{x} \, . \tag{B.4}$$

Transforming integrals back to the reference domain Ω we arrive at a variational characterization of the pullback $\widehat{w}(t) := w(\Omega_t) \circ \mathsf{T}^t_{\boldsymbol{\mathcal{V}}}$: Seek $\widehat{w}(t) \in H^1_0(\Omega)$ such that

$$\widehat{\mathsf{a}}(t; \widehat{w}(t), \widehat{v}) = \widehat{l}_{\widetilde{g}}(t; \widehat{v}) \quad \forall \widehat{v} \in H^1_0(\Omega) \, , \tag{B.5}$$

where, for $\widehat{w}, \widehat{v} \in H^1_0(\Omega)$,

$$\widehat{\mathsf{a}}(t; \widehat{w}, \widehat{v}) := \int_{\Omega} (\mathsf{D}\mathsf{T}^t_{\boldsymbol{\mathcal{V}}}(\widehat{\boldsymbol{x}})^{-\top} \boldsymbol{\nabla} \widehat{w}) \cdot (\mathsf{D}\mathsf{T}^t_{\boldsymbol{\mathcal{V}}}(\widehat{\boldsymbol{x}})^{-\top} \boldsymbol{\nabla} \widehat{v}) |\det \mathsf{D}\mathsf{T}^t_{\boldsymbol{\mathcal{V}}}(\widehat{\boldsymbol{x}})| \, \mathrm{d}\widehat{\boldsymbol{x}} \, , \tag{B.6}$$

$$\widehat{l}_{\widetilde{g}}(t; \widehat{v}) := -\int_{\Omega} \boldsymbol{G}(\mathsf{T}^t_{\boldsymbol{\mathcal{V}}}(\widehat{\boldsymbol{x}})) \cdot (\mathsf{D}\mathsf{T}^t_{\boldsymbol{\mathcal{V}}}(\widehat{\boldsymbol{x}})^{-\top} \boldsymbol{\nabla} \widehat{v}) \, |\det \mathsf{D}\mathsf{T}^t_{\boldsymbol{\mathcal{V}}}(\widehat{\boldsymbol{x}})| \, \mathrm{d}\widehat{\boldsymbol{x}} \, . \tag{B.7}$$

The field energy is also dependent on the parameter t and is given as:

$$\mathcal{E}_F(t) = \widehat{J}(t; \widehat{w}(t)) \, , \quad \widehat{J}(t; \widehat{w}) := \frac{1}{2} \int_{\Omega} \left\| \mathsf{D}\mathsf{T}^t_{\boldsymbol{\mathcal{V}}}(\widehat{\boldsymbol{x}})^{-\top} \boldsymbol{\nabla} \widehat{w}(\widehat{\boldsymbol{x}}) + \boldsymbol{G}(\mathsf{T}^t_{\boldsymbol{\mathcal{V}}}(\widehat{\boldsymbol{x}})) \right\|^2 |\det \mathsf{D}\mathsf{T}^t_{\boldsymbol{\mathcal{V}}}(\widehat{\boldsymbol{x}})| \, \mathrm{d}\widehat{\boldsymbol{x}} \, . \tag{B.8}$$

Following the steps in Section 4.2, we use the adjoint approach [19, §1.6.4] and define the relevant Lagrangian for $\widehat{w}, \widehat{v} \in H^1_0(\Omega)$:

$$L(t; \widehat{w}, \widehat{v}) := \widehat{J}(t; \widehat{w}) + \widehat{\mathsf{a}}(t; \widehat{w}, \widehat{v}) - \widehat{l}_{\widetilde{g}}(t; \widehat{v}) \, . \tag{B.9}$$

Plugging in $\widehat{w} = \widehat{w}(t)$, we recover the expression for field energy

$$\mathcal{E}_F(t) = L(t; \widehat{w}(t), \widehat{v}) \quad \forall \widehat{v} \in H^1_0(\Omega) \, . \tag{B.10}$$

Since we are free to choose $\widehat{v}$, we choose it as the adjoint solution ρ which solves

$$\rho \in H^1_0(\Omega) : \quad \widehat{\mathsf{a}}(0; \widehat{v}, \rho) = -\left\langle \frac{\partial \widehat{J}}{\partial \widehat{w}}(0; \widehat{w}(0)), \widehat{v} \right\rangle \quad \forall \widehat{v} \in H^1_0(\Omega) \tag{B.11}$$

$$\iff \qquad \mathsf{a}(v, \rho) = -\int_{\Omega} (\boldsymbol{\nabla} w + \boldsymbol{G}) \cdot \boldsymbol{\nabla} v \, \mathrm{d}\boldsymbol{x} = 0 \quad \forall v \in H^1_0(\Omega) \, , \tag{B.12}$$

where in the last equality we used (B.1) and the fact that $\widehat{w}(0) = w$. This gives us the adjoint solution $\rho \equiv 0$ and allows us to calculate the shape derivative in terms of partial derivatives of t:

$$\frac{\mathrm{d}\mathcal{E}_F}{\mathrm{d}t}(0) = \frac{\partial L}{\partial t}(0; \widehat{w}(0), \rho) = \frac{\partial \widehat{J}}{\partial t}(0; w) + \frac{\partial \widehat{\mathsf{a}}}{\partial t}(0; w, 0) - \frac{\partial \widehat{\ell}_{\widetilde{g}}}{\partial t}(0; 0) \, . \tag{B.13}$$

The last two terms go to zero and we are left with the partial derivative of $\widehat{J}(0; w)$ defined in (B.8). We can swap integration with the partial derivative and using the required expressions from Section 4.2 we get

$$\frac{\mathrm{d}\mathcal{E}_F}{\mathrm{d}t}(0) = \frac{1}{2} \int_{\Omega} \|\boldsymbol{\nabla} u\|^2 \boldsymbol{\nabla} \cdot \boldsymbol{\mathcal{V}} + 2 \boldsymbol{\nabla} u \cdot (-\boldsymbol{\nabla} \boldsymbol{\mathcal{V}} \boldsymbol{\nabla} u + \boldsymbol{\nabla} \boldsymbol{\mathcal{V}} \boldsymbol{\nabla} \widetilde{g} + \boldsymbol{\nabla} \boldsymbol{\nabla} \widetilde{g} \boldsymbol{\mathcal{V}}) \, \mathrm{d}\boldsymbol{x} \, , \tag{B.14}$$

where we used $w = u - \widetilde{g}$.

References

[1] R. Becker and R. Rannacher. An optimal control approach to *a posteriori* error estimation in finite element methods. *Acta Numer.*, 10:1–102, 2001.

[2] Timo Betcke, Alexander Haberl, and Dirk Praetorius. Adaptive boundary element methods for the computation of the electrostatic capacity on complex polyhedra. *J. Comput. Phys.*, 397, 2019.

[3] A. Bossavit. Forces in magnetostatics and their computation. *J. Appl. Phys.*, 67(9):5812–5814, 1990.

[4] Anthony Carpentier, Nicolas Galopin, Olivier Chadebec, Gérard Meunier, and Christophe Guérin. Application of the virtual work principle to compute magnetic forces with a volume integral method. *Int. J. Numer. Model.*, 27(3):418–432, 2014.

[5] Philippe G. Ciarlet. *Linear and nonlinear functional analysis with applications*. Society for Industrial and Applied Mathematics, 2013.

[6] J. L. Coulomb. A methodology for the determination of global electromechanical quantities from a finite element analysis and its application to the evaluation of magnetic forces, torques and stiffness. *IEEE Trans. Magnetics*, 19(6):2514–2519, 1983.

[7] Monique Dauge. *Elliptic Boundary Value Problems on Corner Domains: Smoothness and Asymptotics of Solutions*, volume 1341 of *Lecture Notes in Mathematics*. Springer, 1988.

[8] Georges de Rham. *Differentiable manifolds. Forms, currents, harmonic forms*, volume 266 of *Grundlehren der Mathematischen Wissenschaften*. Springer, 1984. Translated from the French by F. R. Smith, With an introduction by S. S. Chern.

[9] M. C. Delfour and J.-P. Zolésio. *Shapes and geometries. Metrics, analysis, differential calculus, and optimization*, volume 22 of *Advances in Design and Control*. Society for Industrial and Applied Mathematics, second edition, 2011.

[10] Heiko Gimperlein, Fabian Meyer, Ceyhun Özdemir, David Stark, and Ernst P. Stephan. Boundary elements with mesh refinements for the wave equation. *Numer. Math.*, 139(4):867–912, 2018.

[11] Wei Gong and Shengfeng Zhu. On Discrete Shape Gradients of Boundary Type for PDE-constrained Shape Optimization. *SIAM J. Numer. Anal.*, 59(3):1510–1541, 2021.

[12] P. Grisvard. *Elliptic Problems in Nonsmooth Domains*. Pitman, 1985.

[13] Joachim Gwinner and Ernst P. Stephan. *Advanced boundary element methods*, volume 52 of *Springer Series in Computational Mathematics*. Springer, 2018.

[14] W. Hackbusch. *Integral equations. Theory and numerical treatment.*, volume 120 of *International Series of Numerical Mathematics*. Birkhäuser, 1995.

[15] François Henrotte, G. Deliege, and Kay Hameyer. The eggshell approach for the computation of electromagnetic forces in 2D and 3D. *COMPEL*, 23(4):996–1005, 2004.

[16] François Henrotte and Kay Hameyer. Computation of electromagnetic force densities: Maxwell stress tensor vs. virtual work principle. *J. Comput. Appl. Math.*, 168(1-2):235–243, 2004.

[17] François Henrotte and Kay Hameyer. A Theory for Electromagnetic Force Formulas in Continuous Media. *IEEE Trans. Magnetics*, 43(4):1445–1448, 2007.

[18] Norbert Heuer and Ernst P. Stephan. The *hp*-Version of the Boundary Element Method on Polygons. *J. Integral Equations Appl.*, 8(2):173–212, 1996.

[19] M. Hinze, R. Pinnau, M. Ulbrich, and S. Ulbrich. *Optimization with PDE constraints*, volume 23 of *Mathematical Modelling: Theory and Applications*. Springer, 2009.

[20] Ralf Hiptmair and Jingzhi Li. Shape derivatives in differential forms I: an intrinsic perspective. *Ann. Mat. Pura Appl.*, 192(6):1077–1098, 2013.

[21] Ralf Hiptmair, A. Paganini, and S. Sargheini. Comparison of approximate shape gradients. *BIT Numer. Math.*, 55:459–485, 2014.

[22] J. D. Jackson. *Classical electrodynamics*. John Wiley & Sons, 3rd edition, 1998.

[23] Matthias Maischak and Ernst P. Stephan. The *hp*-version of the boundary element method in $\mathbb{R}^3$: The basic approximation results. *Math. Methods Appl. Sci.*, 20:461–476, 1997.

[24] S. McFee, J. P. Webb, and D. A. Lowther. A tunable volume integration formulation for force calculation in finite-element based computational magnetostatics. *IEEE Trans. Magnetics*, 24(1):439–442, 1988.

[25] W. McLean. *Strongly Elliptic Systems and Boundary Integral Equations*. Cambridge University Press, 2000.

[26] J.-C. Nédélec. *Acoustic and Electromagnetic Equations: Integral Representations for Harmonic Problems*, volume 44 of *Applied Mathematical Sciences*. Springer, 2001.

[27] F. H. Read. Improved Extrapolation Technique in the Boundary Element Method to Find the Capacitances of the Unit Square and Cube. *J. Comput. Phys.*, 133(1):1–5, 1997.

[28] S. Sauter and C. Schwab. *Boundary Element Methods*, volume 39 of *Springer Series in Computational Mathematics*. Springer, 2010.

[29] J. Sokolowski and J.-P. Zolésio. *Introduction to shape optimization*, volume 16 of *Springer Series in Computational Mathematics*. Springer, 1992.

[30] Olaf Steinbach. *Numerical approximation methods for elliptic boundary value problems*. Springer, 2008.

[31] Ernst P. Stephan. The *hp*-version of BEM – Fast convergence, adaptivity and efficient preconditioning. *J. Comput. Math.*, 27(2-3):348–359, 2009.